# NAVAL POSTGRADUATE SCHOOL
## Monterey, California

# THESIS

---

**A FEASIBILITY STUDY OF OSCILLATING-WING POWER GENERATORS**

by

Keon Lindsey

September 2002

Thesis Advisor:                    Kevin D. Jones
Second Reader:               Max F. Platzer

---

**Approved for public release; distribution is unlimited**

THIS PAGE INTENTIONALLY LEFT BLANK

| REPORT DOCUMENTATION PAGE | | *Form Approved OMB No. 0704-0188* |
|---|---|---|

Public reporting burden for this collection of information is estimated to average 1 hour per response, including the time for reviewing instruction, searching existing data sources, gathering and maintaining the data needed, and completing and reviewing the collection of information. Send comments regarding this burden estimate or any other aspect of this collection of information, including suggestions for reducing this burden, to Washington headquarters Services, Directorate for Information Operations and Reports, 1215 Jefferson Davis Highway, Suite 1204, Arlington, VA 22202-4302, and to the Office of Management and Budget, Paperwork Reduction Project (0704-0188) Washington DC 20503.

| 1. AGENCY USE ONLY *(Leave blank)* | 2. REPORT DATE September 2002 | 3. REPORT TYPE AND DATES COVERED Master's Thesis | |
|---|---|---|---|
| 4. TITLE AND SUBTITLE: A Feasibility Study of Oscillating-Wing Power Generators | | 5. FUNDING NUMBERS | |
| 6. AUTHOR(S) Lindsey, Keon | | | |
| 7. PERFORMING ORGANIZATION NAME(S) AND ADDRESS(ES) Naval Postgraduate School Monterey, CA 93943-5000 | | 8. PERFORMING ORGANIZATION REPORT NUMBER | |
| 9. SPONSORING /MONITORING AGENCY NAME(S) AND ADDRESS(ES) N/A | | 10. SPONSORING/MONITORING AGENCY REPORT NUMBER | |

11. SUPPLEMENTARY NOTES  The views expressed in this thesis are those of the author and do not reflect the official policy or position of the Department of Defense or the U.S. Government.

| 12a. DISTRIBUTION / AVAILABILITY STATEMENT Approved for public release; distribution is unlimited | 12b. DISTRIBUTION CODE |
|---|---|

13.  ABSTRACT *(maximum 200 words)*

Mankind is continually searching for new sources of energy or methods to harness known sources.  Recently, renewable and zero-pollution energy supplies are of great interest.  Consequently, power generation from a fluttering wing is studied numerically and experimentally.  Previous studies have suggested that an oscillating-wing used to extract energy from a fluid flow could deliver power comparable to windmills.  Several studies are examined.  An oscillating-wing power generator is designed and tested.  The experimental results are compared with numerical predictions.  Finally, commercial applications of the "environmentally friendly" oscillating-wing generator are investigated.

| 14. SUBJECT TERMS Oscillating-Wing, Flutter, Wingmill, Power Production, Power Extraction, Aerodynamics, Generator, Clean Energy, Numerical Modeling, Laplace, Navier-Stokes | | | 14.  NUMBER OF PAGES 81 |
|---|---|---|---|
| | | | 16. PRICE CODE |
| 17. SECURITY CLASSIFICATION OF REPORT Unclassified | 18. SECURITY CLASSIFICATION OF THIS PAGE Unclassified | 19. SECURITY CLASSIFICATION OF ABSTRACT Unclassified | 20. LIMITATION OF ABSTRACT UL |

i

THIS PAGE INTENTIONALLY LEFT BLANK

**A FEASIBILITY STUDY OF OSCILLATING-WING POWER GENERATORS**

Keon Lindsey
Lieutenant, United States Navy
B.S., United States Naval Academy, 1994


Submitted in partial fulfillment of the
requirements for the degree of


**MASTER OF SCIENCE IN AERONAUTICAL ENGINEERING**


from the


**NAVAL POSTGRADUATE SCHOOL**
**September 2002**


Author:          Keon Lindsey


Approved by:     Kevin D. Jones
                 Thesis Advisor


                 Max F. Platzer
                 Second Reader/Co-Advisor


                 Max F. Platzer
                 Chairman, Department of Aeronautics and Astronautics


iii

THIS PAGE INTENTIONALLY LEFT BLANK

# ABSTRACT

Mankind is continually searching for new sources of energy or methods to harness known sources. Recently, renewable and zero-pollution energy supplies are of great interest. Consequently, power generation from a fluttering wing is studied numerically and experimentally. Previous studies have suggested that an oscillating-wing used to extract energy from a fluid flow could deliver power comparable to windmills. Several studies are examined. An oscillating-wing power generator is designed and tested. The experimental results are compared with numerical predictions. Finally, commercial applications of the "environmentally friendly" oscillating-wing generator are investigated.

THIS PAGE INTENTIONALLY LEFT BLANK

# TABLE OF CONTENTS

THIS PAGE INTENTIONALLY LEFT BLANK

# LIST OF FIGURES

THIS PAGE INTENTIONALLY LEFT BLANK

# LIST OF TABLES

THIS PAGE INTENTIONALLY LEFT BLANK

# LIST OF SYMBOLS

$A$      area swept out by a wing

$b$      effective wing span

$c$      chord length

$Cp$      power coefficient, $2P / \rho_\infty V_\infty^2 S V_\infty$

$\overline{Cp}$      time averaged power coefficient

$D$      drag

$f$      oscillation frequency in Hertz

$h$      plunge amplitude in terms of $c$

$k$      reduced frequency, $\omega c / V_\infty$

$P$      power in Watts, $1/2 \rho_\infty A V_\infty^3$

$\overline{P}$      time averaged power

$S$      wing area, $bc$

$t$      time

$V_\infty$      freesteam velocity in m/s

$\omega$      circular frequency of oscillation, $2\pi f$

$W$      Watts power

$x_p$      pivot point

$y(t)$      vertical displacement in terms of $c$

$y^+$      dimensionless normal wall distance

$\alpha$      angle of attack in degrees

$\Delta\alpha$      sinusoidal pitch amplitude

$\Gamma$    circulation

$\phi$    phase angle in degrees

$\rho_\infty$    freestream density

$\eta$    propulsive efficiency

$\eta_{PD}$    drag based efficiency, $P/DV_\infty$

$\eta_{total}$    total efficiency, $\overline{C}p / Cp_{available}$

# ACKNOWLEDGMENTS

THIS PAGE INTENTIONALLY LEFT BLANK

# I. INTRODUCTION

## A.    BACKGROUND

Aeronautical engineers have been examining the concept of flutter for some time now.  This is due to the potentially catastrophic consequences that result from an aircraft wing fluttering in flight.  Under the right conditions a wing will begin to oscillate, pitching and plunging as it absorbs energy from flowing air.  Naturally, when an aircraft's wing begins to oscillate, the structure may be damaged.  However, an unattached wing with proper damping may be constrained to pitch and plunge, without harm to itself, and allowed to extract energy from the flow.

Currently, windmills and hydroelectric generators extract energy from fluids flowing past rotary devices.  Since a fluttering wing is also extracting energy from a flowing fluid, it warrants investigation as a power generator.  Issues that such an inquiry must consider are, the mechanics of a constraining mechanism, the efficiency of such a device, and how much energy can actually be extracted from the flow.

McKinney and Delaurier [Ref. 1] built a device, which they called a *wingmill*, and made the first known test of oscillating-wing power generation.  Their work suggests that a wingmill could compete with conventional windmills in generating power.   Jones and Platzer [Ref. 2] performed a numerical analysis for flapping-wing power generation with an Unsteady Potential Code (UPOT).  Their study found that if pitch amplitude exceeding the induced angle of attack due to the plunging motion and the phase between pitch and plunge was such that, pitch led plunge by approximately 90 degrees, then an oscillating-wing would indeed be suitable for some power generation application.

Thus, Davids [Ref. 3] set out to verify Jones and Platzer's prediction.  He first used UPOT to investigate what combination of parameters would give optimum performance, and then tested a device (provided by Jones and Platzer) in a water tunnel. Davids' work showed that the key to maximizing output was a proper combination of oscillation frequency and plunge amplitude.  However, the single-wing experimental device had some unforeseen limitations, which led Davids to suggest improvements for further study.

**B.      OVERVIEW**

More recently, Dr. Kevin Jones designed a two-wing wingmill.  His device is the one that this study used for experimental data.   Prior to conducting tests, numerical analysis was performed with UPOT to (1) duplicate Davids' results and (2) with a modified version of UPOT survey a larger field of parameters than Davids was able to do to find optimum combinations.   Since UPOT is based on the solution to the Laplace equation, which assumes irrotational, incompressible flow modeled by summing solutions from simple flows, this study also took advantage of a Navier-Stokes (NS) based numerical code, which made fewer limiting assumptions.     Once optimum parameters were found with UPOT, NS was used to probe for solutions near those parameters (since NS is much more expensive to run).  Dr. Jones' device was then tested with the NS determined parameters of frequency and plunge amplitude to check for agreement, as well as, a broader range for future study purposes.

**C.      APPLICATION**

The oscillating-wing generator has demonstrated its ability to deliver power. Now the search for applications is in order.  Davids suggested it might compete with micro-hydro generators or be used in the same manner as hydroelectric power stations but without requiring a dam.  The micro generators are capable of producing enough electricity to supply the demands of a small energy efficient household.  A micro version of an oscillating-wing generator can deliver as much as, and more power than a commercial generator of the same size.  Hydroelectric power stations supply enough energy to run several communities.  An oscillating-wing generator in the same class as a power plant generator would be capable of delivering comparable energy without restricting traffic on waterways.  While the new power generator species can compete with existing ones, the major question remains how well can it compete in the cost category.

## II.  FLUTTER THEORY

There are three phenomena that typically act on a an aircraft's wing within a flow, aerodynamic forces, elastic reactions, and inertia.  The interaction between these three can cause the wing to flutter under certain conditions.  This fluttering is actually the result of the wing absorbing energy.  If the wing is properly coupled to harness its pitch and plunge, its motion may be used to extract energy from the flow.

The aerodynamic forces, which impinge on an airfoil, result from pressure (normal force) and shear stress (tangential force) distributed over the surface of the body. [Ref. 4]  The force may be resolved into the familiar components of lift and drag, along with a moment.  Lift pulls a body upward (perpendicular to the freestream), drag pulls it aft (parallel to the freestream), and the moment causes it to pitch.  The wing will transfer these forces to the aircraft—causing it to fly.

The elastic reaction of a wing section is simply the material responding to the aerodynamic forces.  As force is applied to a body, it must move or be deformed.  A body that is able to sustain stress (to a certain degree) without permanent deformation is termed elastic. [Ref. 5]  For example, when an aircraft wing develops lift, the wing bends upward.  As long as it is not overstressed, the wing will return to its original shape once lift generation ceases.  This is why large aircraft wings appear to be bowed upward in flight, they actually are.

Inertia is described by Newton's First Law of Motion.  It is the tendency of a body at rest to remain at rest and of a body in motion to remain in motion unless a force acts upon it to change the state.

These three phenomena interact as fluids flow over airfoils.  Consider the response of aircraft wings.  Aerodynamic forces pull and pitch wings in flight.  The wings' elastic reaction is to bend and twist respectively.  Inertia causes the wings' bending and twisting to continue until some limit is reached.  According to Platzer,

> It is quite possible that when several degrees of freedom are present, a phase relation may develop that results in a positive energy input into the airfoil…. It is seen that positive work is done on the airfoil when the

3

torsional deflection leads the bending deflection…by about 90 degrees….
Thus, different combinations of wing motion lead to phase shifts, which
enable the wing to extract energy from the airstream and become 'self-
propagating'. This is the basic mechanism which causes flutter. [Ref. 6]

If the airflow is fast enough and the system damping sufficiently small the self-
excitation or fluttering will begin to diverge rapidly until the wings are ripped off or self-
destruct from not being able to absorb all of the energy that causes these oscillations.
This destructive tendency is largely avoided in aircraft by limiting their operating speeds,
but it is the ability to harness this energy that leads to the concept of a flutter or
oscillating-wing generator.

An oscillating-wing's motion must be describable in mechanical terms if energy
is to be harnessed from it. In two dimensions the wing's movement may be constrained
in such a fashion as to have only two components. Its up and down motion will be
referred to as plunge, and twisting as pitch. Pitch and plunge have the same frequency
and are coupled by a phase angle. The phase angle will determine how much, if any,
work is done on the airfoil, and thus, how much energy is extracted from the flow. The
work produced at phase angles of zero and 90 degrees is illustrated in Figure 1. In both
cases the dashed arrows represent airfoil motion and the solid arrows show lift. In Case
1, pitch and plunge are 90 degrees out of phase with pitch leading. Recall that work is
force times distance. Since the lift force and the motion are always in the same direction,
work is positive all the time. In Case 2, pitch and plunge have the same phase. Thus,
when the airfoil motion is upward, its pitch is also positive. This means that during part
of the cycle, lift and motion are in the same direction, producing positive work and
during the other part they are opposing, producing negative work. So the net work
throughout a cycle with zero phase difference is zero, because the positive and negative
work cancel.

Case 1: Phase difference 90 Degrees. Positive Work all the time.



Case 2: Phase difference 0 Degrees. Net Work Zero.
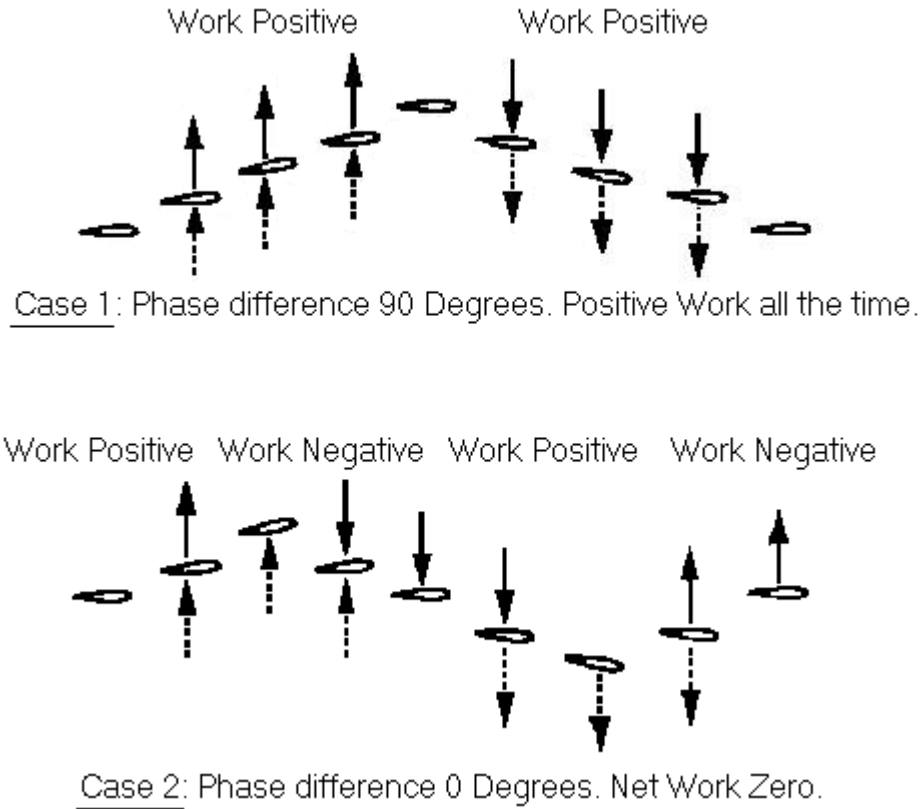
Figure 1.    Phase Relationship of Pitching and Plunging Airfoil. After Ref. 6.

As mentioned earlier, the aerodynamic forces on an oscillating airfoil are not constant.  The changes in lift are of particular interest at this point.  As the airfoil plunges through the flow, the instantaneous lift that it experiences differs from the quasi-steady lift.  "The quasi-steady lift is the lift force induced by the plunging motion of the airfoil if the plunge velocity were constant." [Ref. 3]   The difference arises from the flow "remembering" the disturbances that result from the airfoil's change of orientation (aerodynamic forces do not change instantaneously with airfoil alignment).   The aerodynamic disturbances are remembered in vortices, shed from the airfoil, traveling downstream in the flow.  These vortices will affect the circulation around the airfoil. "Circulation is the negative of the line integral of velocity of a closed curve in the flow." [Ref. 4]  It is denoted by $\Gamma$, and seen in equation form as

$$\Gamma = -\int_c \mathbf{V} \cdot \mathbf{ds} \qquad (1)$$

Whenever an airfoil changes orientation the circulation around it changes. "When the circulation changes, the Helmholtz Theorem states that there must be an equal and opposite reaction in the flow. This reaction takes the form of a vortex shed into the flow by the airfoil called a starting vortex." [Ref. 3] If an airfoil is in continuous motion it will constantly shed vorticity, which will influence its performance until it is dissipated somewhere downstream. This vorticity will figure prominently in any wingmill analysis.

## A.  PERFORMANCE PARAMETERS

The parameters that will be considered during the investigation of an oscillating-wing generator are Reduced Frequency, Plunge Amplitude, Pitch Amplitude, Phase Angle, and Pivot Point.  For the numerical modeling in this study, the pitching and plunging motions are assumed to be sinusoidal, described by

$$y(t) = h\sin(kt + \phi) \qquad (2)$$

$$\alpha(t) = \Delta\alpha\sin(kt) \qquad (3)$$

Reduced frequency is the nondimensionalized rate of recurrence of wingmill motion.  It is defined as

$$k = \frac{\omega c}{V_\infty} \qquad (4)$$

where $\omega$ is the circular frequency of oscillation $\omega = 2\pi f$, $c$ is the chord length, and $V_\infty$ is the freestream velocity. Plunge amplitude, $h$, is the distance of the airfoil's motion, measured in chord lengths with zero being at neutral.  It is defined at the pivot location, thus, it is not necessarily the vertical distance covered by the airfoil.  Pivot point is measured in chord lengths from the leading edge.  Phase angle, $\phi$, describes the lead or lag between pitch and plunge.  Pitch amplitude expresses the size of change in angle of attack and is denoted by $\Delta\alpha$.  The geometric and induced angles of attack determine the effective angle of attack as seen in Figure 2.
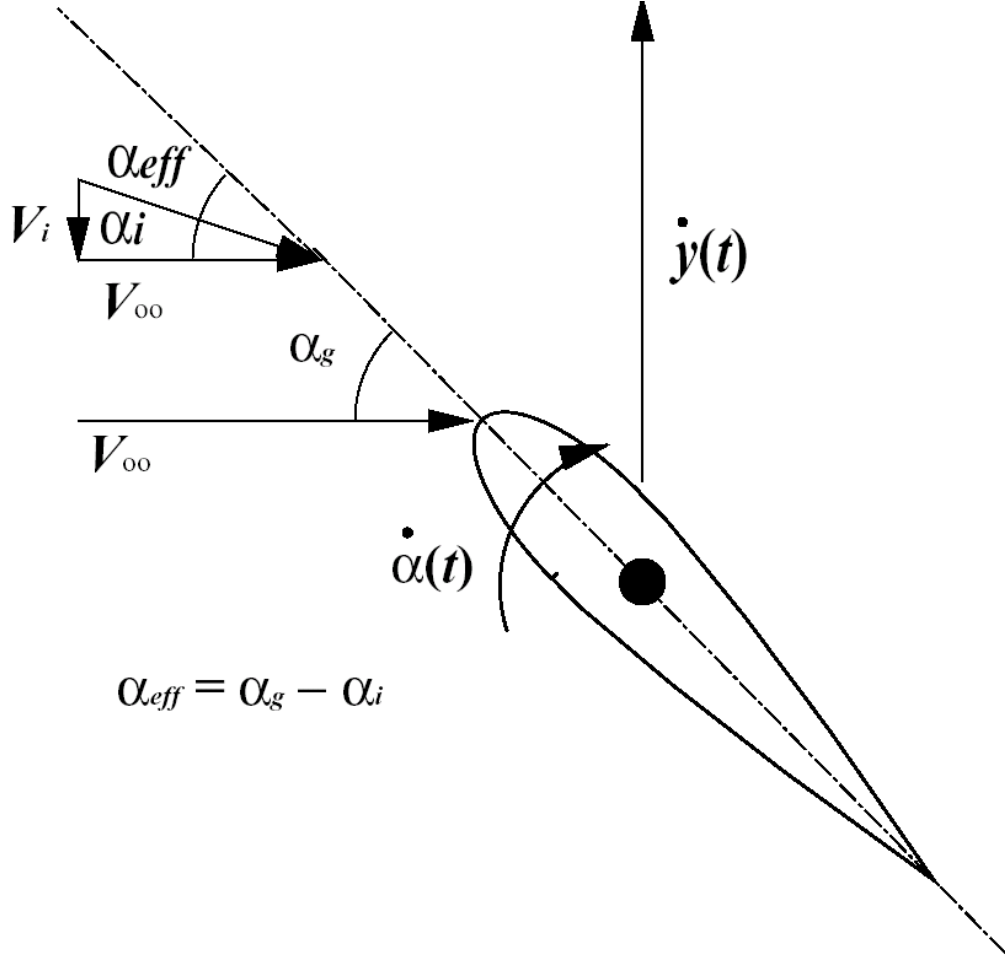
Figure 2.   Effective Angle of Attack.  After Ref. 3.

Of particular interest is the effective angle of attack at the leading edge of the moving wing.  It is there that dynamic flow separation often begins, which means it may give indications as to when in the pitch-plunge cycle the airfoil can no longer extract power from the flow.  The leading edge effective angle of attack is defined by

$$\alpha_{eff} = \alpha(t) - \tan^{-1}\left[\frac{\dot{y}(t) - \dot{\alpha}(t)x_p\cos(\alpha(t))}{V_\infty - \dot{\alpha}(t)x_p\sin(\alpha(t))}\right] \qquad (5)$$

As seen in equation (5), this effective angle of attack is significantly impacted by pitch rate if $x_p$ is not close to zero.

## B.    PERFORMANCE MEASURES

The above parameters will impact the wingmill's performance, which will be measured in terms of the coefficient of power, $C_p$, and efficiency, $\eta$. $C_p$ is defined as

$$C_p = \frac{P}{\frac{1}{2}\rho_\infty V_\infty^2 S V_\infty} \qquad (6)$$

where $P$ is power extracted from the flow, $\rho_\infty$ is the freestream density, $V_\infty$ is the freestream speed, and $S$ is the wing planform area.  Basic fluid mechanics relates the maximum power available to a device such as a windmill (and by extension, a wingmill) as the time rate of change of kinetic energy in the flow, or

$$P_{available} = \frac{1}{2}\rho_\infty A V_\infty^3 \qquad (7)$$

where $A$ is the area of the actuator disk or the area swept out by the wingmill.  Actuator Disk Theory predicts the highest total efficiency that a windmill may achieve is 16/27, which is known as the Betz Coefficient. [Ref. 10]

In studies on propulsion, efficiency is generally defined as the ratio of propulsive power (thrust times velocity) to power input into the system.  For energy extraction from flowing fluids, efficiency is the reciprocal of the propulsive case, or

$$\eta_{PD} = \frac{P}{DV} \qquad (8)$$

with thrust being replaced by drag, $D$.  This efficiency, based on drag, is optimal when drag is minimal or when the flow is only slightly disturbed.  Drag-based efficiency might be appropriate for oscillating-wing generators if several airfoils were placed in a series each extracting a small amount of energy from the flow, much like a turbine.

Efficiency may also be defined as total or ideal.  Total efficiency is a measure of the power extracted compared to the power contained in the flow.  Ideal efficiency is a measure of the power extracted compared to the power that it is *possible* to extract from the flow.  Thus, for a mechanism that extracts power from a flowing fluid, its highest achievable total efficiency is 16/27 or 59.3%, as shown above.  However, if the same

device can actually remove all 59.3% of the extractable power from that flow, it will have an ideal efficiency of 100%. This study will use total efficiency defined by

$$\eta_{total} = \frac{\bar{P}_{out}}{P_{available}} = \frac{\bar{C}_p}{C_{p,available}} \qquad (9)$$

where $\bar{P}_{out}$ and $\bar{C}_p$ are the time averaged quantities over one or more cycles.

THIS PAGE INTENTIONALLY LEFT BLANK

# III. INVESTIGATION OF PREVIOUS WORK

## A.     MCKINNEY AND DELAURIER

McKinney and Delaurier set out to study "the feasibility of a windmill consisting of a rigid horizontal wing oscillating in plunge (vertical translation) and pitch." [Ref. 1] Their theoretical analysis used unsteady-wing aerodynamics from aeroelasticity. It "identified the important nondimensional parameters for the wingmill's power production, which included: 1) reduced frequency; 2) plunge amplitude/wing chord; 3) pitch amplitude; 4) lift-curve slope; 5) wing area/actuator area; 6) phase angle." [Ref. 1]

Their experiment yielded an average power 19% greater than the analytical prediction. McKinney and Delaurier found that at lower phase angles theory and experiment matched very well, however, as phase angle increased theory and experiment began to diverge. This was attributed to dynamic-stall-delay effects, which allowed their airfoil to generate lift at angles of attack higher than those analytically anticipated. They measured an ideal efficiency of 28.3% (total efficiency of 16.8%), which "was surprisingly high". This was determined to be a result of "the fact that airfoil normal forces dominate in the power-production cycle", and therefore, more lift leads to more power. McKinney and Delaurier's work demonstrated "that the wingmill idea is mechanically realizable, and that it is capable of producing power at efficiencies which are competitive with other designs." [Ref. 1]

## B.     JONES AND PLATZER

In Jones and Platzer's work, "Numerical methods were described for the systematic computation of unsteady, inviscid, incompressible, two-dimensional flows about moving airfoils" and applied "to the investigation of flapping-wing propulsion and power extraction." They observed that for single mode motions, either pitching or plunging, there was agreement between linear theory for small frequencies and amplitudes. However, as frequency and amplitude increased, so did the difference between numerical methods and linear theory. [Ref 2]

For a dual mode flapping wing Jones and Platzer determined that if the pitch-amplitude was "increased sufficiently it was found that drag was produced and power was extracted from the airfoil….For this to occur the pitch amplitude must exceed the induced angle of attack due to the plunging motion, and the phase between pitch and plunge is restricted to a range near 90 degrees." This work validated the previous claim that a wingmill may actually be a power extraction device worth pursuing. [Ref. 2]

While Jones and Platzer agree with McKinney and Delaurier, the more important contribution was a method for further study and prediction of wingmill capabilities before another experiment was conducted.

C.    DAVIDS

Davids built on the work of Jones and Platzer with the goal of performing an experimental wingmill analysis. In his study "computational and experimental methods [were] used to investigate the possibility of extracting power from a flow using an oscillating airfoil." He used an unsteady panel code to determine the combination of parameters that resulted in optimum performance efficiency from a wingmill. Davids examined a range of reduced frequencies, plunge amplitudes, pivot locations, phase angles, and angles of attack. He chose an effective angle of attack of 15 degrees, for which he determined the optimum reduced frequency to be 1.975, plunge amplitude 0.625, pivot location at 0.55 m.a.c., and phase angle as 94 degrees for a NACA 0012 airfoil. This combination yielded the peak efficiency of 30.01%. From the numerical analysis, Davids concluded that maximum performance hinged on the proper combination of plunge amplitude, $h$, and reduced frequency, $k$. [Ref. 3]

Davids went on to test a wingmill provided by Jones at his predetermined parameters. He was unable to reach the predicted total efficiency due to mechanical limitations of the device (his were on the order of 15%), however, the information he collected suggested that the numerical trends were correct.

# IV.  METHODS OF ANALYSIS

Flutter analysis may be accomplished numerically or experimentally.  Two methods of numerical analysis were available for this study.  Computer programs allowed a potential flow analysis to be performed and provided solutions for the Navier-Stokes equation.  The results were compared to determine the limitations and compatibilities of each code.  Further, an experimental device was constructed to verify the computational claims.

## A.  UPOT ANALYSIS

The Unsteady Potential Code or UPOT was originally developed by Teng. [Ref. 7]  "The technique extends the well known Panel Methods for steady flow into solving a non-linear unsteady flow problem arising from the continuous vortex shedding into the trailing wake due to the unsteady motion of the airfoil."  [Ref. 7]  Panel methods are based on the Laplace equation, which governs two-dimensional incompressible flow over an arbitrary airfoil at an angle of attack.  Laplace allows complicated flow patterns to be synthesized by summing a number of simple irrotational and incompressible flows.  Davids covers UPOT's use of panels and Laplace thoroughly.  However, these methods are limited by the underlying assumptions (see introduction) and may not be sufficient for the desired analysis.  Thus, to develop unlimited results, another method is necessary.  Despite its limitations, UPOT's primary benefit is its low expense calculations, allowing for a broad field survey of the parameter space.

## B.  NAVIER-STOKES ANALYSIS

Flow over an airfoil may be studied using the Navier-Stokes (NS) equation without having to make as many "restrictive" assumptions as UPOT.  However, since there are fewer restrictions, the calculations are quite expensive.  To handle the NS equation, the differential equations are replaced with finite differences.  The differences are resolved on a grid, which yields better approximations as the size of its cells are

reduced. In actuality, phenomena, which are smaller than a grid cell cannot be resolved, and may end up being lost in what might be called "numerical viscosity".

One method that sped up solving the equations was the thin layer approximation. This approximation says that the viscous terms of the NS equations are contained in a thin layer oriented in the direction of the surface. Its basis is that boundary layer viscous terms in the vertical direction are orders of magnitude larger than those in the direction that parallels the flow. Also, Reynolds averaging is used for high Reynolds Number flows. This technique employs turbulence modeling since the numerical grid used in NS codes cannot resolve the actual turbulence due to its size.

This study ran one set of NS calculations at a Reynolds Number of $10^6$ and a second set at $2 \times 10^4$. The first case simulated a large-scale application but the lower Reynolds Number case was necessary to model the flow that would be found in the water tunnel tests. The computational grid used for the high Reynolds Number case is displayed in Figure 3. Initial spacing at the wall is roughly $1 \times 10^{-5} c$, yielding a $y^+$ value of approximately 1. Figure 4 is a close up of the grid from Figure 3. The low Reynolds Number grid with an initial spacing of $1 \times 10^{-4} c$ is seen in Figure 5. Figure 6 is a close up of the grid from Figure 5. The different grid sizes were required to capture (as best as possible) the details of the flows.
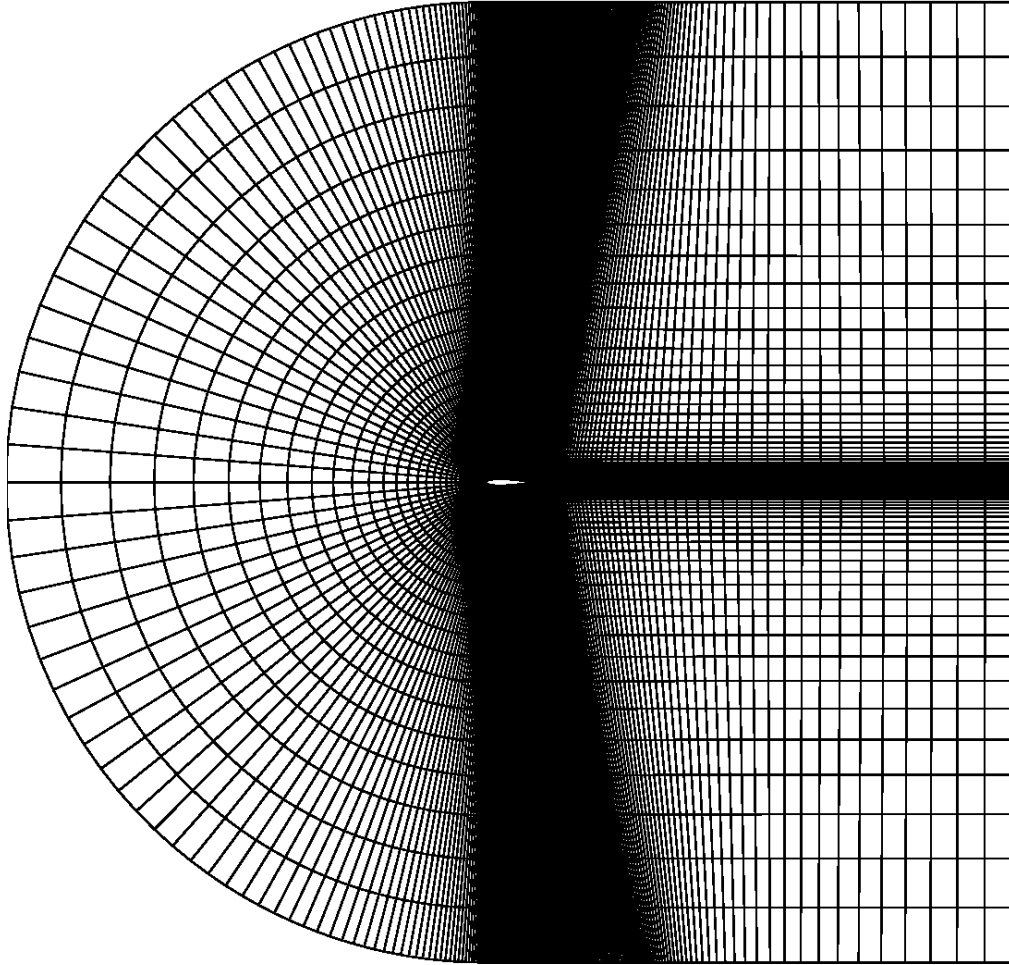
Figure 3.    Computational Grid for Reynolds Number $10^6$ Navier-Stokes Analysis
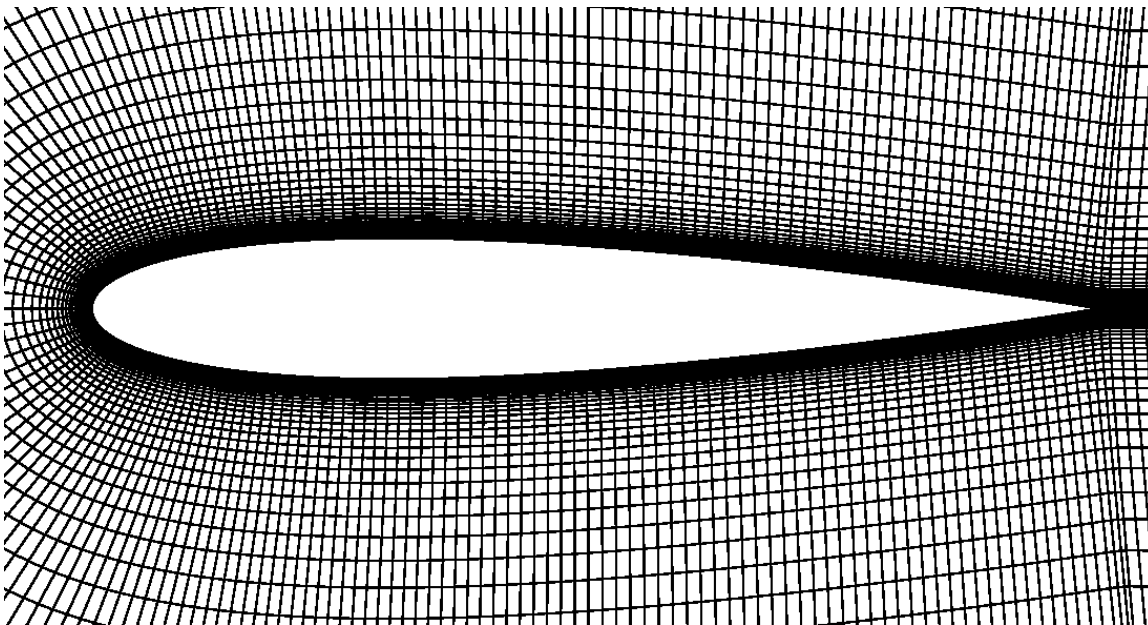


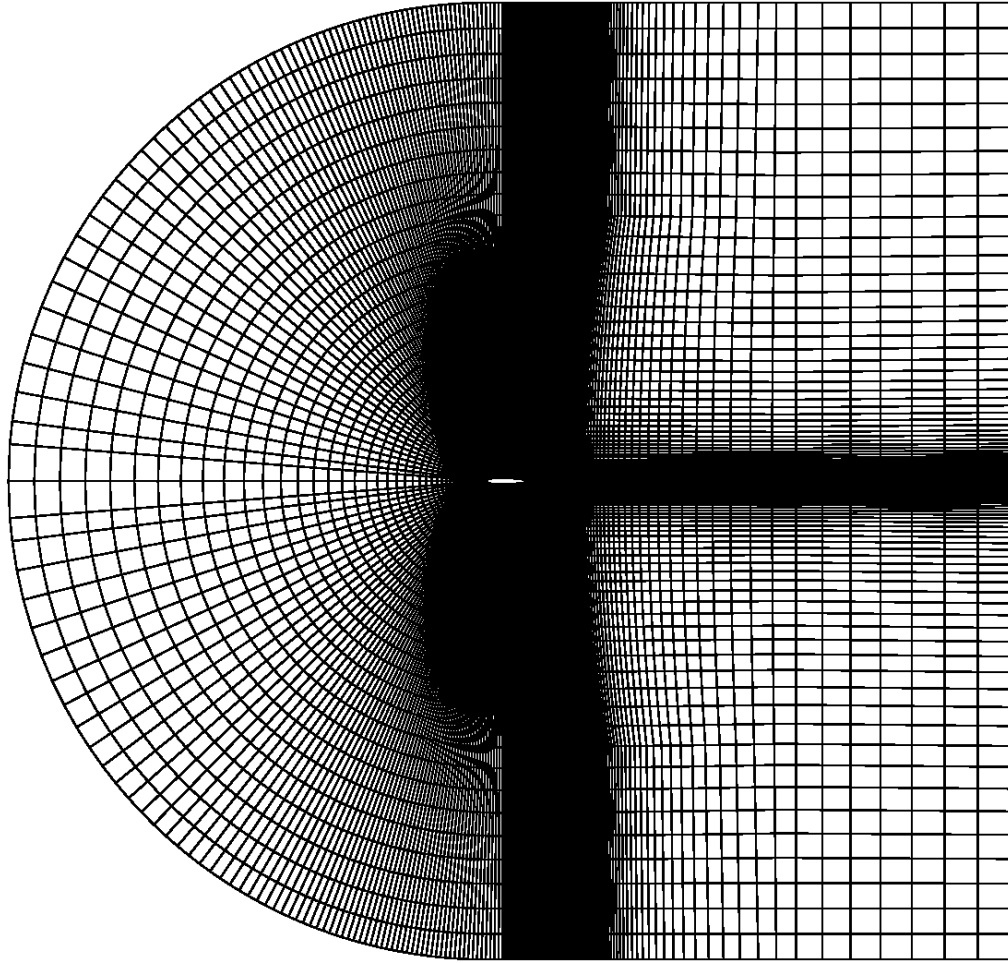Figure 4.    Close Up View of the High Reynolds Number Grid

Figure 5.    Computational Grid for Reynolds Number $2x10^4$ Navier-Stokes Analysis
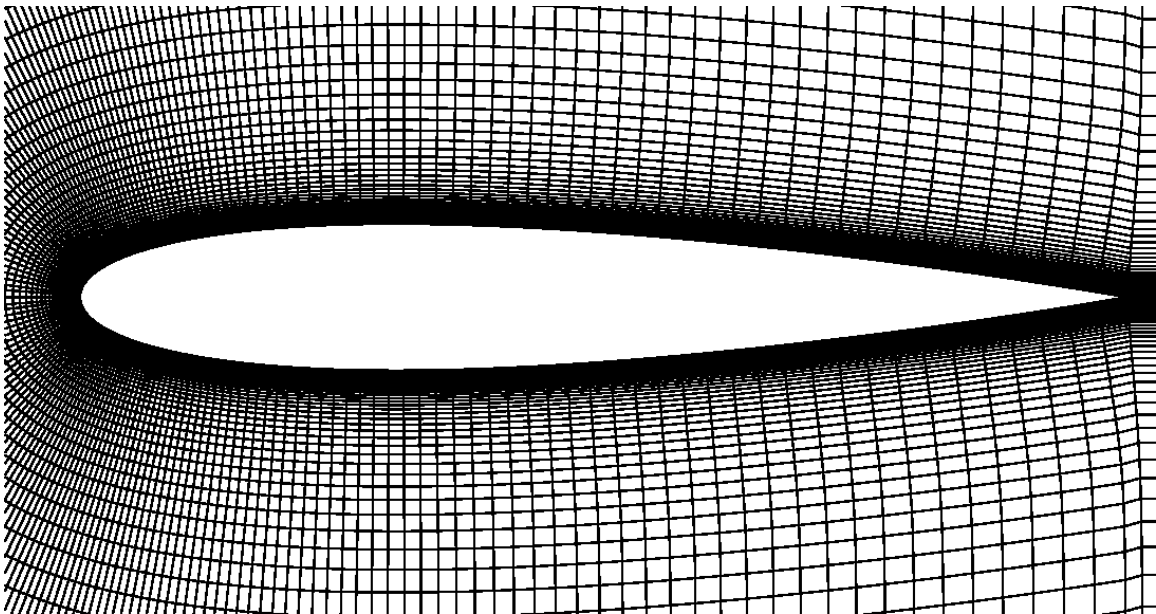


Figure 6.    Close Up View of the Low Reynolds Number Grid

The NS code used for this study employs the Baldwin-Lomax Turbulence Model and was developed by Ekaterinaris and Menter et. al. [Ref. 8] It may be used to simulate unsteady, compressible, three-dimensional viscous flows. This study sought specific performance parameters involving oscillating wings, so UPOT first provided the "general" solution space, then the NS code was used to further refine the solutions.

## C.    EXPERIMENTAL ANALYSIS

One focus of this study was to determine the combination of phase, oscillation frequency, plunge amplitude, etc. (will be discussed later) which would give optimal power and efficiency from a flutter generator. To that end, the previously mentioned numerical methods were used to survey the field of parameters. Then the flutter generator designed by Dr. Kevin Jones of the Naval Postgraduate School was used to resurvey that field in hopes of verifying the numerical results.

### 1.  Apparatus

As mentioned, Jones' oscillating-wing generator employs two wings. It is designed for water tunnel testing and uses a Prony brake (named for G. C. F. M. Riche, Baron de Prony (1755-1839), a French hydraulic engineer [Ref. 9]) for power dissipation. The device is capable of varying oscillation frequency, plunge amplitude, phase, and airfoil pitching point. As a result, it could operate at the predicted optimal conditions, as well as, others. Figure 7 is an engineering drawing of the generator in the water tunnel test section.
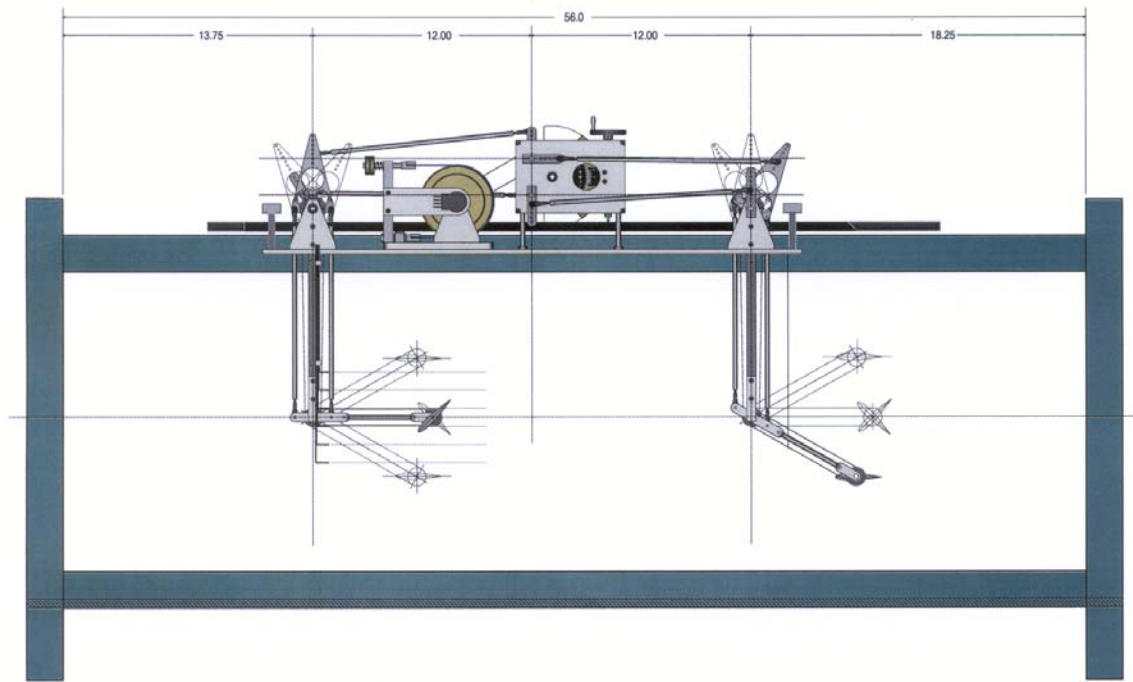
Figure 7.    Jones' Oscillating-Wing Power Generator in a Water Tunnel Test Section

Figure 8 is a close up of the rocker arm assembly.  The airfoil section utilized is approximated by a NACA 0014 with a chord length of 2.5 inches and semi-span of 6.75 inches (two wing sections were connected side by side on each arm, as wings would be attached to a fuselage).  The flapping wing is seen to be at zero angle of attack at its maximum and minimum plunge.  It reaches maximum pitch at neutral plunge.  This is accomplished by means of toothed pulleys and timing belts.  The airfoil is capable of reaching pitch amplitudes of $\pm 88.5$ degrees.  The rocker arm moves the plunge pushrods seen in the left of the picture.  The airfoil's plunge amplitude is controlled through the geometry of pushrods and bellcranks pictured in Figure 8.  The plunge amplitude may also be increased by installing longer rocker arms.
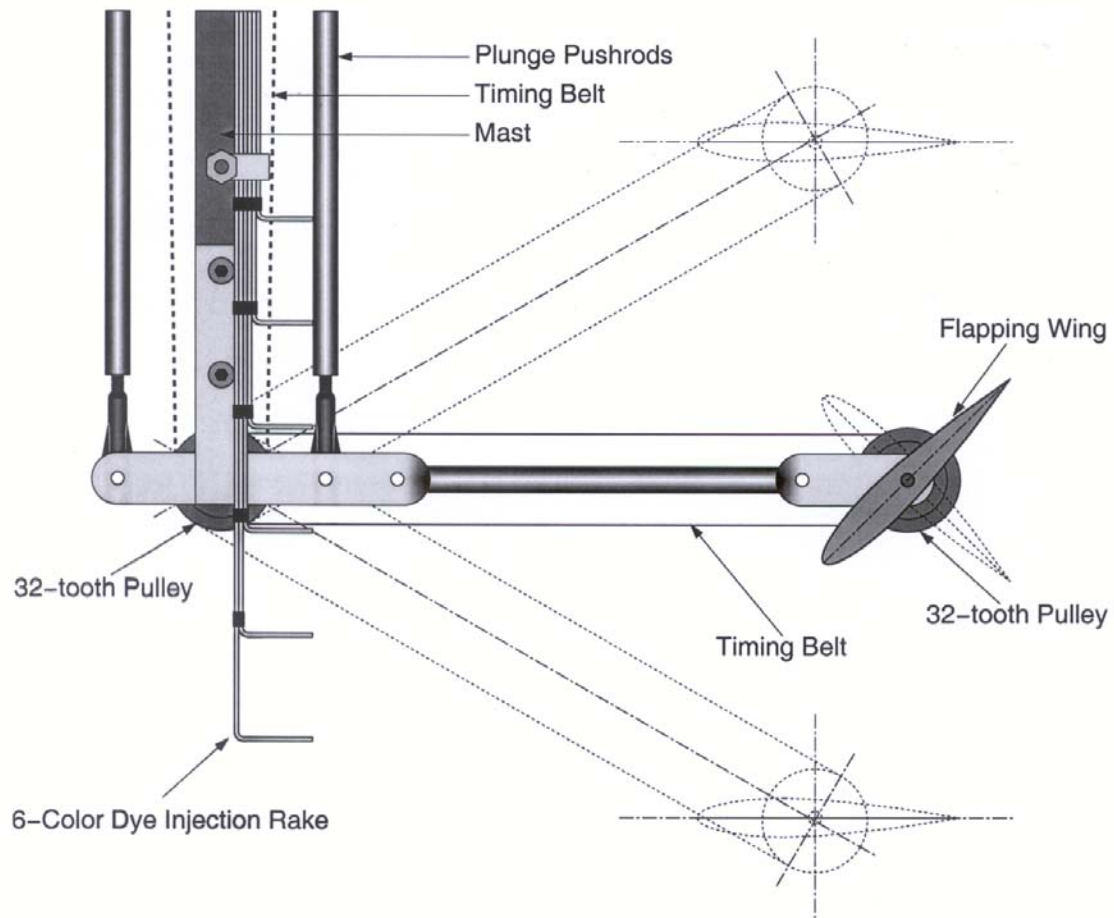
Figure 8.    Close up view of Oscillating-wing Rocker Arm Assembly

Figure 9 is a detailed view of the masthead assembly.  It is here that the vertical motion of the plunging airfoil is translated into horizontal motion en route to the power extraction device.  The plunge pushrods tilt a bellcrank fore and aft, which turns a wheel to convert translational motion into rotational.  The timing belt and toothed pulley cause the pitch bellcrank to tilt fore and aft, which also turns a wheel.  The wheels mentioned here are spun by the actuator arms shown in Figure 10, which also pictures the phase adjustment mechanism.

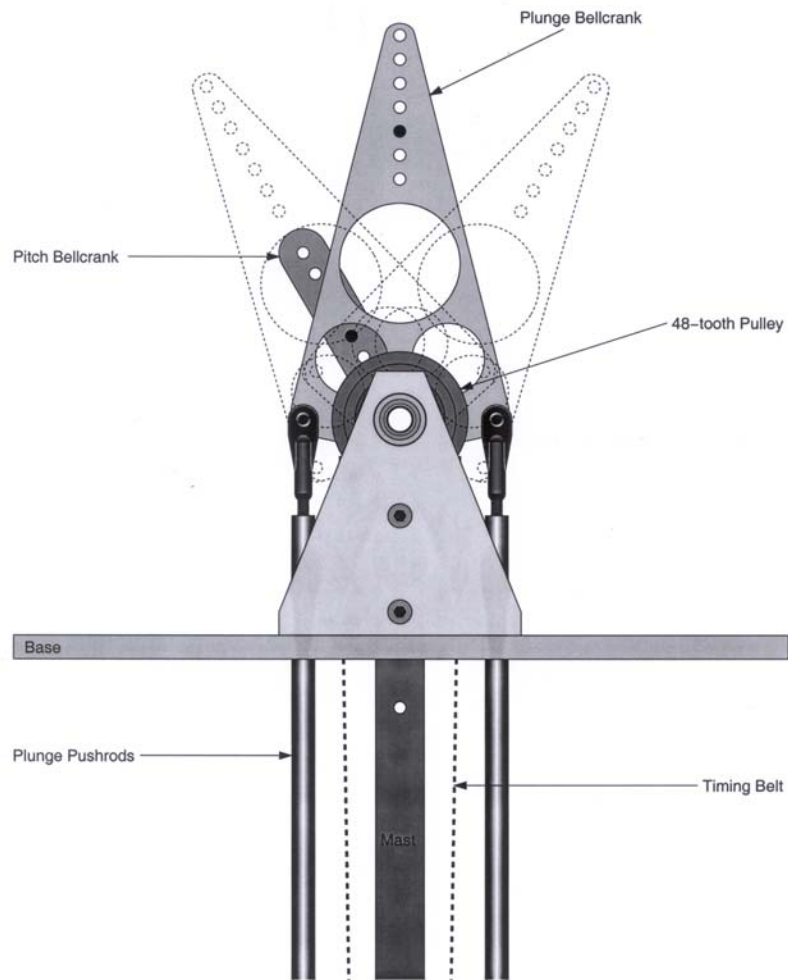Figure 9. Detailed view of the Generator's Masthead Assembly
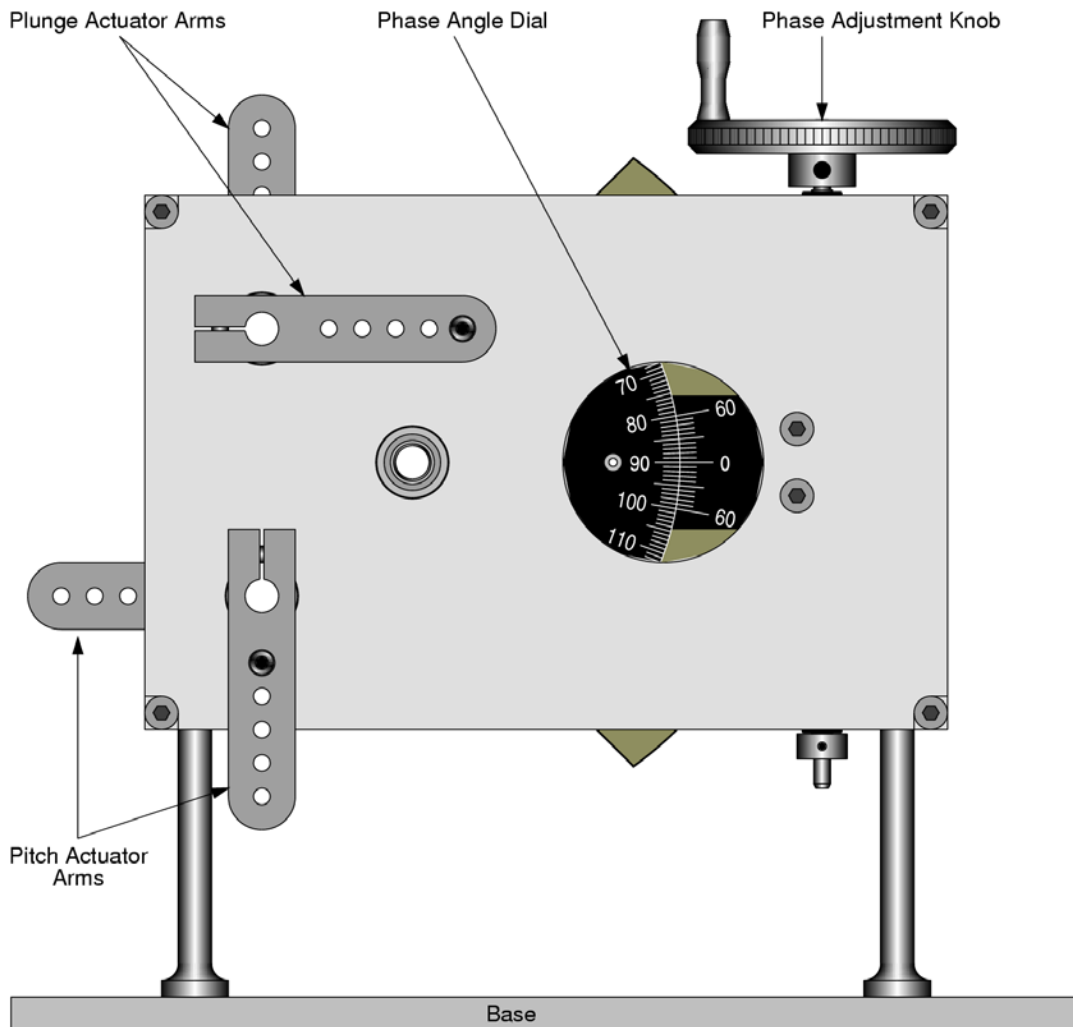
Figure 10. Close up view Actuator Arms and Phase Adjuster


In Figure 11 the pieces of the oscillating-wing power generator are put together and pictured up close. The Prony brake and strain gauge for power measurement are seen in the box labeled "Instrumentation Assembly". Tension on the brake is controlled by a spring and adjustable screw at the opposite end of the friction belt from the strain gauge. In that same box the optical rotary encoder is pictured at the center of the flywheel. The encoder measures the flywheel's position, which when compared to time, provides rotational velocity. The flywheel occupies the place where an electrical generator could be mounted. Its inertial effects help improve the smoothness of the device's power stroke.

Figure 11.   Front half of the Experimental Generator

## 2.  Water Tunnel

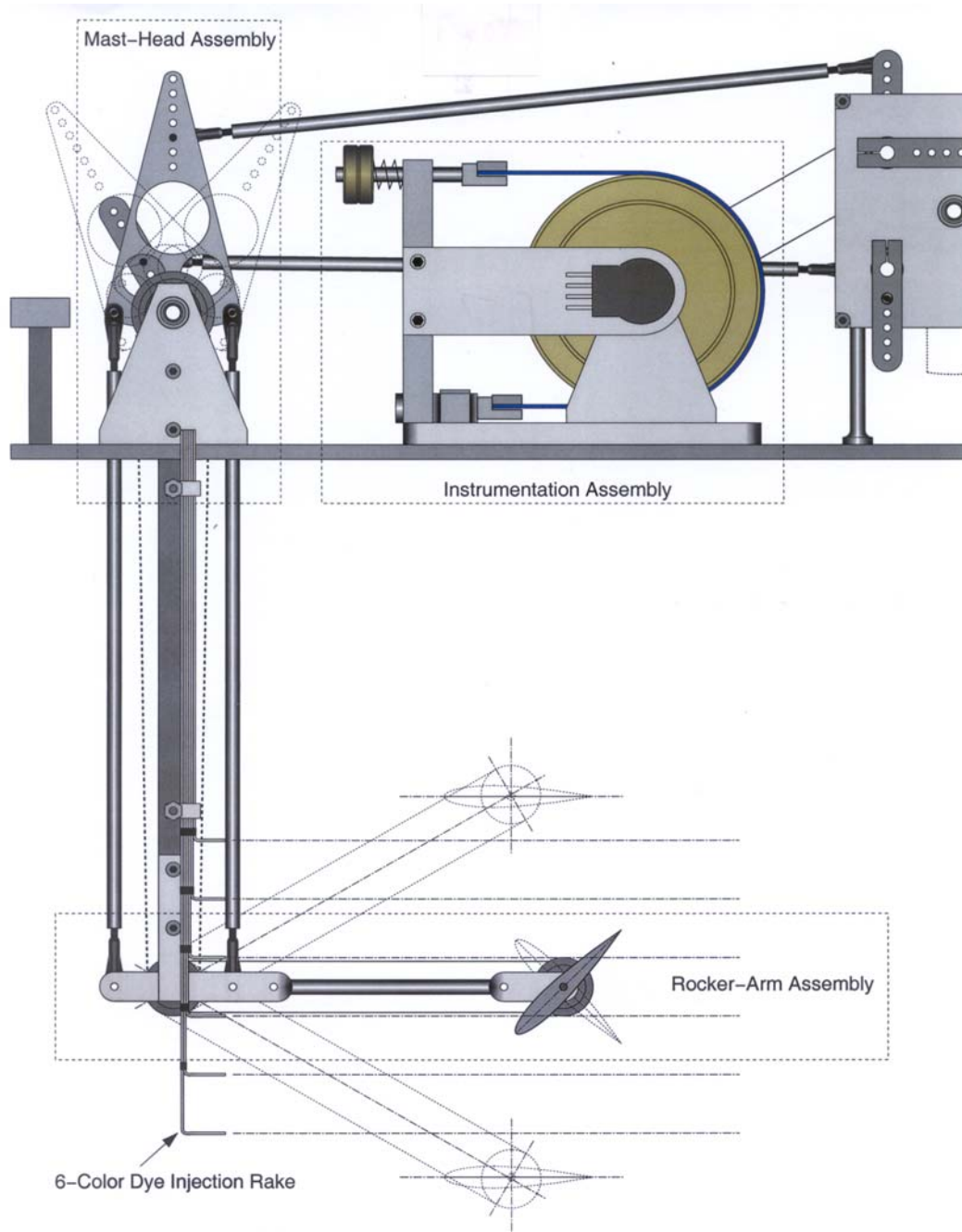The experimental apparatus was operated in the water tunnel at the Naval Postgraduate School Department of Aeronautics.   The tunnel is a closed circuit continuous flow system with horizontal orientation.  Its water flow velocity ranges from 0

to 16 inches per second and is controlled by a variable speed pump with electronic control. Water passes through a honeycomb upstream to remove disturbances before it reaches the test section. The test chamber is 15 inches wide, 56 inches long, and nominally 20 inches deep.

### 3. Description of Test

Jones' oscillating-wing power generator was operated in various configurations in the water tunnel. Each configuration tested began with no friction load on the Prony brake and the water flowing at 16 inches per second so that the free oscillation velocity could be recorded. Next, tension was increased on the friction device until the generator ceased motion, then it was slightly reduced to obtain minimum movement. This condition corresponded to the maximum power extraction regime and minimum oscillation frequency. Five samples of dynamic rotational and strain (for torque and power calculation) data were taken. Then the water flow was stopped and five static strain measurements were taken. In between each static measurement the generator arms were moved a short distance so that the strain gauge would be disturbed and allowed to resettle. After this, the cycle was repeated four additional times. Each successive cycle used a lower tension (corresponding to lower power extracted) to obtain a higher oscillation frequency approaching the unrestricted case. Data was collected in 16 second increments to be time averaged, typically covering 14-18 cycles.

Successive configurations tested would have either a different geometric angle of attack or new plunge amplitude. The end result was data covering a range of frequencies for several pitch amplitudes at each plunge amplitude. With the tunnel at maximum speed, a Reynolds number of 22,274 was achieved.

An attempt was made to visualize what happened in the flow around and between the two flapping wings by injecting dye into the water upstream of the first wing. However, at 16 inches per second the dye rake shed a vortex street that quickly dissipated the dye. The tunnel could be operated at lower speeds where streamlines were visible but that was too slow for the generator to run. Due to time constraints, the other option of emitting dye from the surface of the airfoil, was not possible at the time.

23

## 4. Sources of Error

Errors for which a measurement was possible are described first. One source of error for the conducted tests is in the water tunnel speed measurements. A water flow calibration was provided with the tunnel, however, there was not a device available to verify it. Therefore, a small fluctuation of 0.25 inches per second was assumed, which would not affect the measured power and frequency but would impact $C_p$ and $k$. The frictional force of the belt proved to be inconsistent introducing uncertainty into power measurements. An attempt to estimate this possible error was made by averaging several data sets and taking the standard deviation as the error. The neutral and powered tension of the Prony brake were each sampled five times then averaged to obtain best representative values, again using the standard deviation for the error. In calibrating the strain gauge a least squares curve fit was used, which also is representative, but not exact, and the standard deviation was assumed here as well. Finally, the cycle-to-cycle variations in friction and power throughout the experiment were also addressed with averaging. The error measurements are summed in quadrature and shown with error bars in the data plots.

Some issues were not addressed by the numerical models. These included the differences between two and three-dimensional flow. Also, the codes were not designed to consider the effects of the aft wing operating in the wake of the forward wing.

Some errors were beyond the ability of this study to consider, although they are noted here. Alignment of the airfoils on the generator in the zero angle of attack position was estimated and may cause up to 3 degrees of variation from the desired angle. Misalignment of airfoils may yield power production for angles of attack not specified. This may introduce significant errors if operating near the region of dynamic stall. Defects in the model wings are left for future production improvement. Error in plunge amplitude was neglected. Friction within the experimental model is unknown. Also, it was not known how much inertia from moving parts or added mass from the rocker arms displacing water impacted measurements. The interference between masts and moving wings (including the gap between wings on the same arm) was not estimated. Finally,

extra play in the pitch and plunge motions due to machining and tolerance errors in the device were not addressed.

THIS PAGE INTENTIONALLY LEFT BLANK

# V. NUMERICAL RESULTS

## A.     UPOT

The UPOT investigation began with a sensitivity analysis to determine how many computation cycles, steps per cycle, and number of panels should be used for the panel code to give acceptable results without using unnecessary amounts of time.  In the graphs below, where each parameter is plotted against average $C_p$, the "knee" in the curve indicates a point beyond which computations will cost too much time in return for very little improvement in accuracy.  Thus, this study used 15 cycles, 60 steps per cycle, and a 50 panel per surface airfoil for UPOT research.  It should be noted that since UPOT is inviscid and incompressible, the Reynold's Number is effectively infinity and the Mach number is effectively zero.
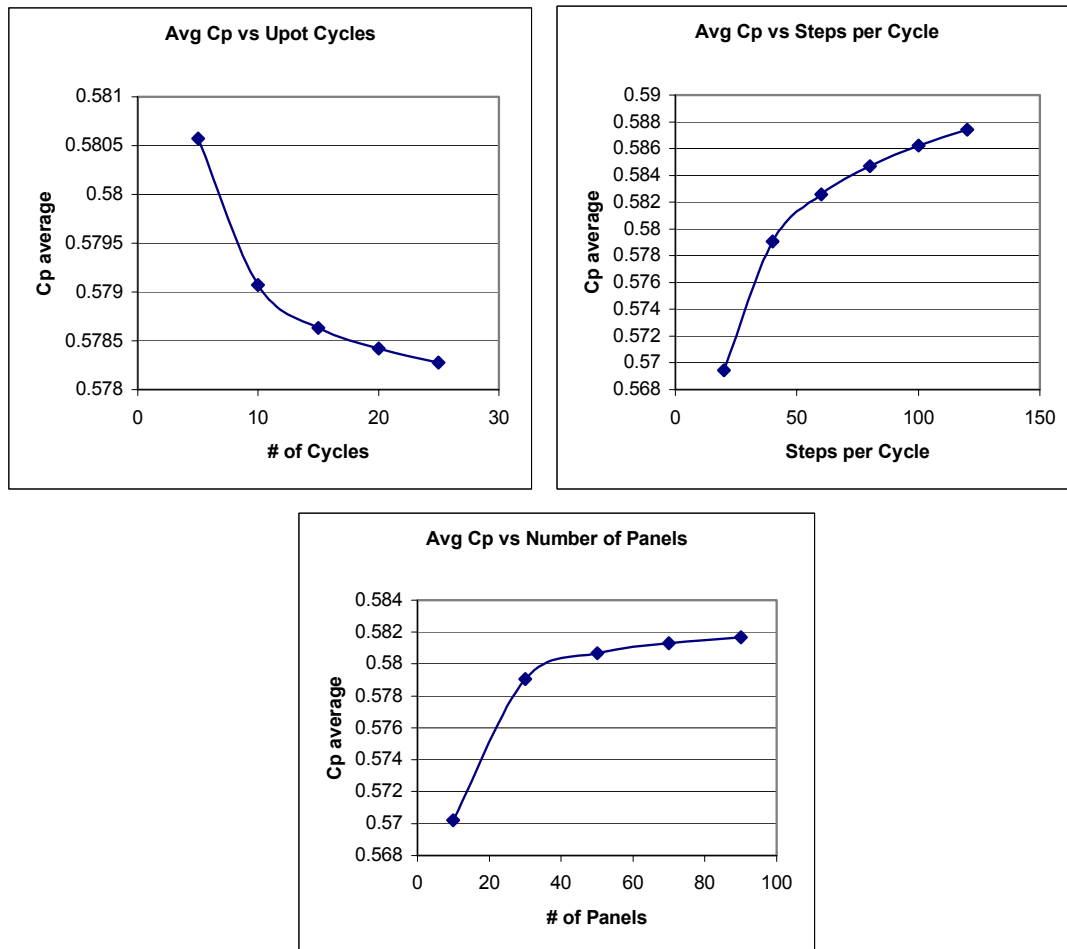


Figure 12.   UPOT Sensitivity Analysis

27

Thanks to a UPOT modification provided by Jones, this study was able to survey a wide range of parameters relatively quickly. This numerical investigation chose values of effective angle of attack, phase angle, and pivot point to determine the power and efficiency resulting from an airfoil oscillating through a reduced frequency range from zero to four and amplitudes between zero and five. It began with Davids optimal values of effective angle of attack at 15 degrees, phase angle of 90 degrees, and pivot point at 55% chord, then deviated to determine how power and efficiency were affected. Peak performance in power and efficiency are shown in the topographical features of the figures in this section.

It should be noted that the first thing UPOT demonstrated was its range of useful application in frequency and plunge amplitude domain. In the middle of the investigation described above, the code returned some remarkable numbers. As seen in Figure 13, UPOT returned a total efficiency greater than one, which is impossible.
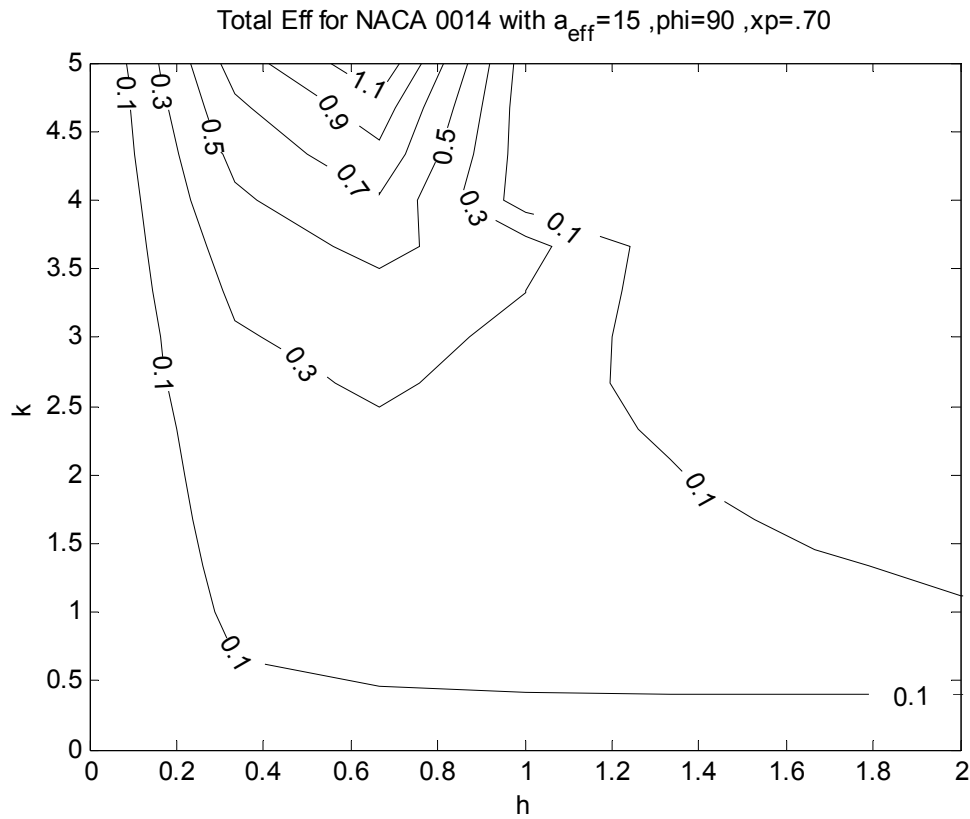


Figure 13. Example of UPOT Limits: Efficiency Greater than 1 for High Values of *k*.

28

Jones determined that at high frequencies UPOT's estimated induced angle of attack exceeded 180 degrees. The impossible efficiency resulted from the code's approximations for induced angle of attack due to plunge

$$\alpha_{ind_y}(t) = \tan^{-1}\left(\frac{y'(t)}{V_\infty}\right) \qquad (10)$$

and from the approximated effective angle of attack

$$\alpha_{eff}^* = \alpha(t) - \alpha_{ind_y}(t) \quad (11)$$

Comparison of the true effective angle of attack, Equation (5) repeated here,

$$\alpha_{eff} = \alpha(t) - \tan^{-1}\left[\frac{\dot{y}(t) - \dot{\alpha}(t)x_p\cos(\alpha(t))}{V_\infty - \dot{\alpha}(t)x_p\sin(\alpha(t))}\right] \qquad (5)$$

and UPOT's estimate, Equation 11 will reveal the extent of possible error in the approximation, although it is correct if the pivot point is at the leading edge. Figure 14 illustrates the differences between the approximation of effective angle of attack and the true angle. The estimate gets farther from the actual as pivot point moves farther aft.
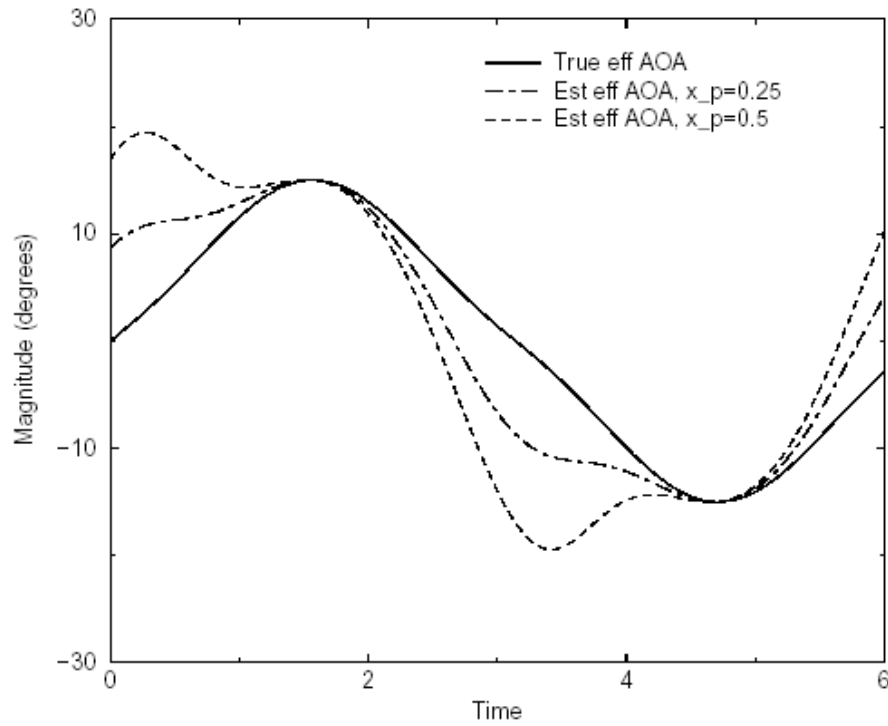


Figure 14. Leading Edge Effective Angle of Attack. $\Delta\alpha = 15°$, k=0.7, h=1, $\phi = 90°$

29

In such extreme cases described above, non-physical phenomena were present, such as vorticies propagating through the airfoil. The code was modified to discard the erroneous solutions by skipping them if *hk* was greater than 4 or if the effective angle of attack exceeded 90 degrees at any point in the cycle. These were arbitrary limits, however, since UPOT was primarily used to show trends, the important object was to filter the obvious mistakes. This interesting discovery led to the realization that UPOT's reliability was restricted to *k* values of roughly two or less for problems of this type. With this new knowledge, a trustworthy examination could begin in earnest using UPOT.

### 1. Changes in Phase Angle

The study used UPOT to examine phase angles from 80 to 110 degrees. The results reveal that as phase angle increases power decreases although total efficiency improves. As the amount by which pitch leads plunge grows, peak power extracted from the flow shifts from low reduced frequency and higher plunge amplitude to higher frequencies and lower amplitudes. This trend is seen in Figure 15.
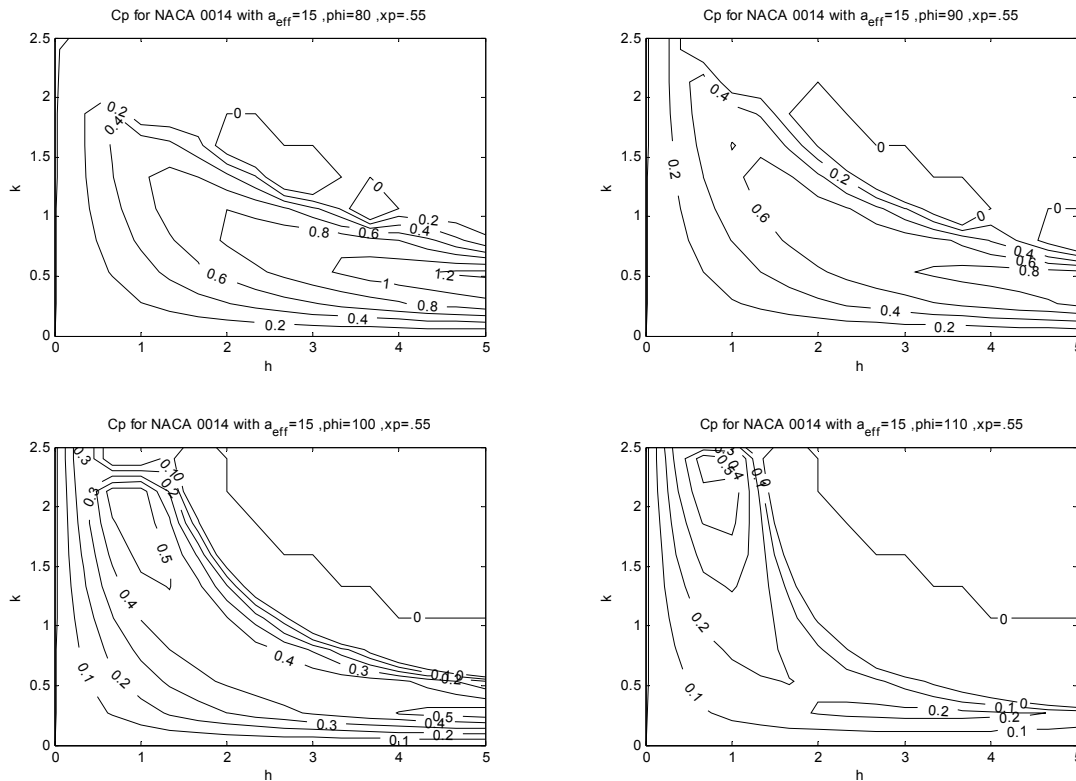


Figure 15. Changes in Power with Phase Angle

The position of peak total efficiency remains relatively constant, in the region of low plunge amplitude with slightly higher reduced frequency, as shown in Figure 16. There is only a slight increase in efficiency as phase angle increases, however, it does appear to plateau at 100 degrees, and even that is in UPOT's questionable range for $(hk)_{max}$.
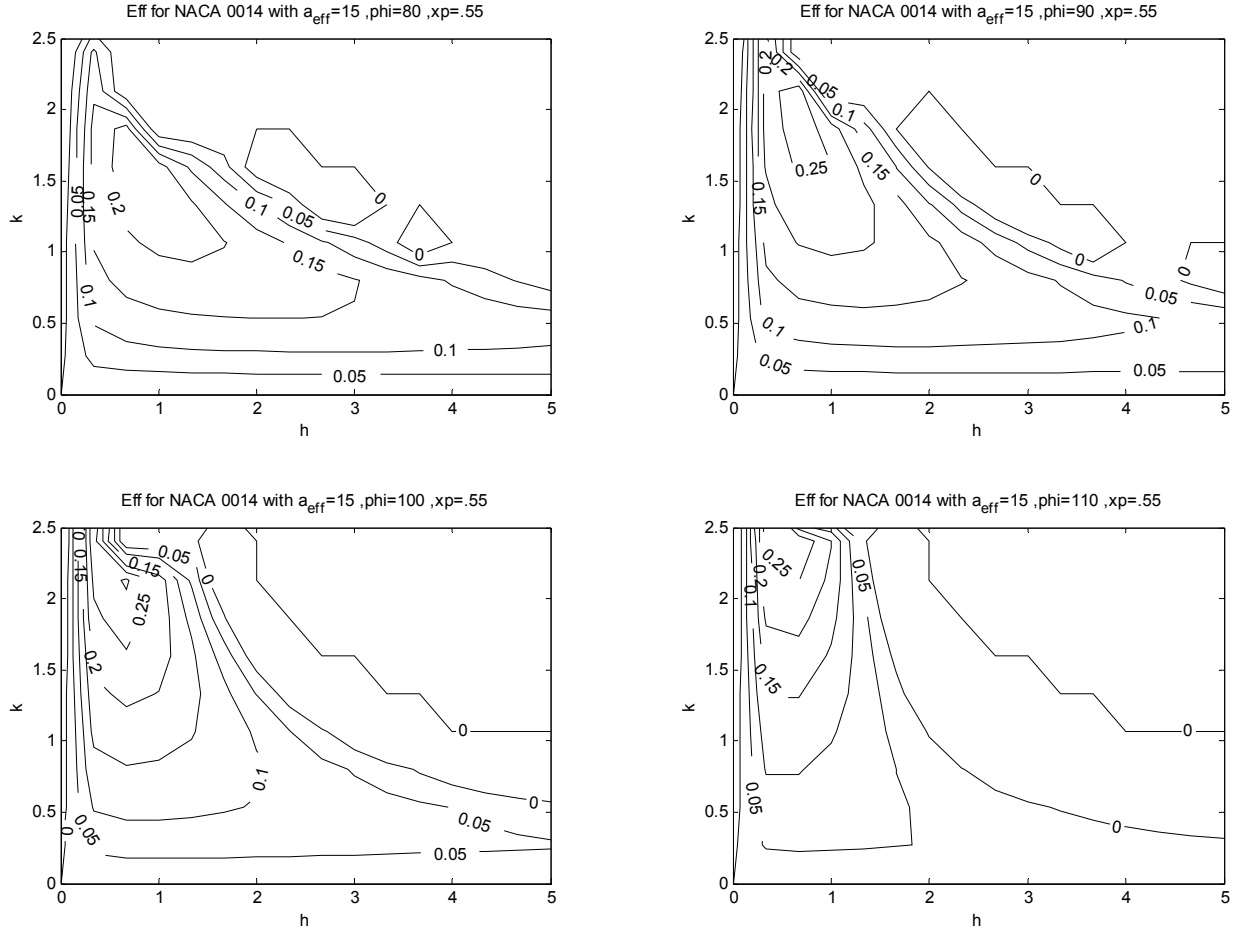


Figure 16.   Changes in Total Efficiency with Phase Angle

## 2. Changes in Pivot Point

As the airfoil pivot point moved aft from 12.5% to 80% of the chord, peak power decreased. As seen in Figure 17, maximum power out is obtained at higher plunge amplitudes and low reduced frequencies.
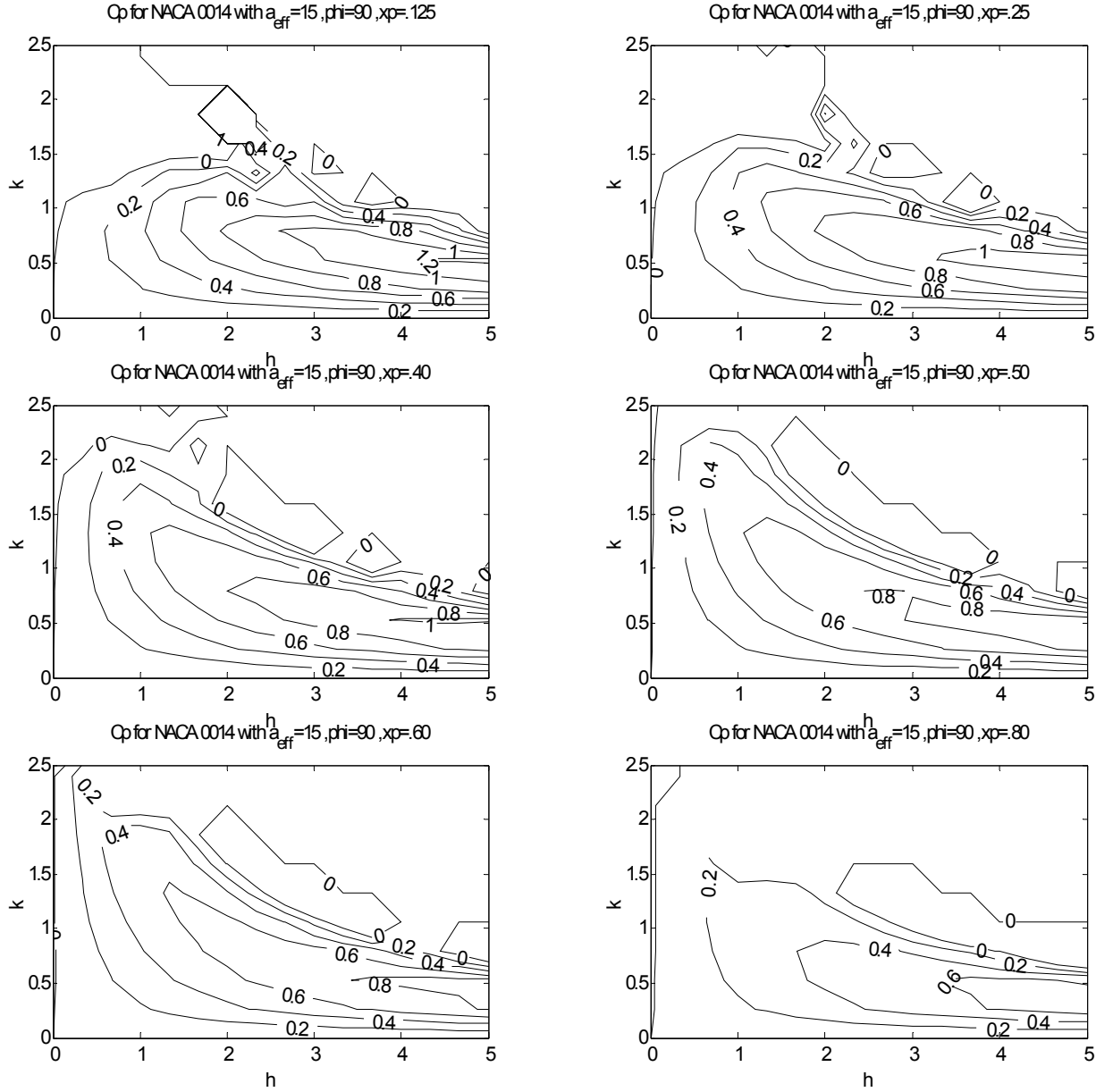


Figure 17. Changes in Power with Pivot Point

In Figure 18 it may be seen that efficiency increases until the airfoil pivots near midchord then falls off. This trend results from swept area being minimized when the pivot point is at midchord. It also illustrates the movement of peak efficiency from low reduced frequency and plunge amplitude near two times the chord, to slightly higher frequency and lower amplitude, then back towards the original parameters.

Figure 18.   Changes in Total Efficiency with Pivot Point

### 3. Changes in Effective Angle of Attack

UPOT does not give the user the option to set an effective angle of attack. Instead, the code would take the desired effective angle of attack and, through Equation 11, approximate the geometric angle of attack that would 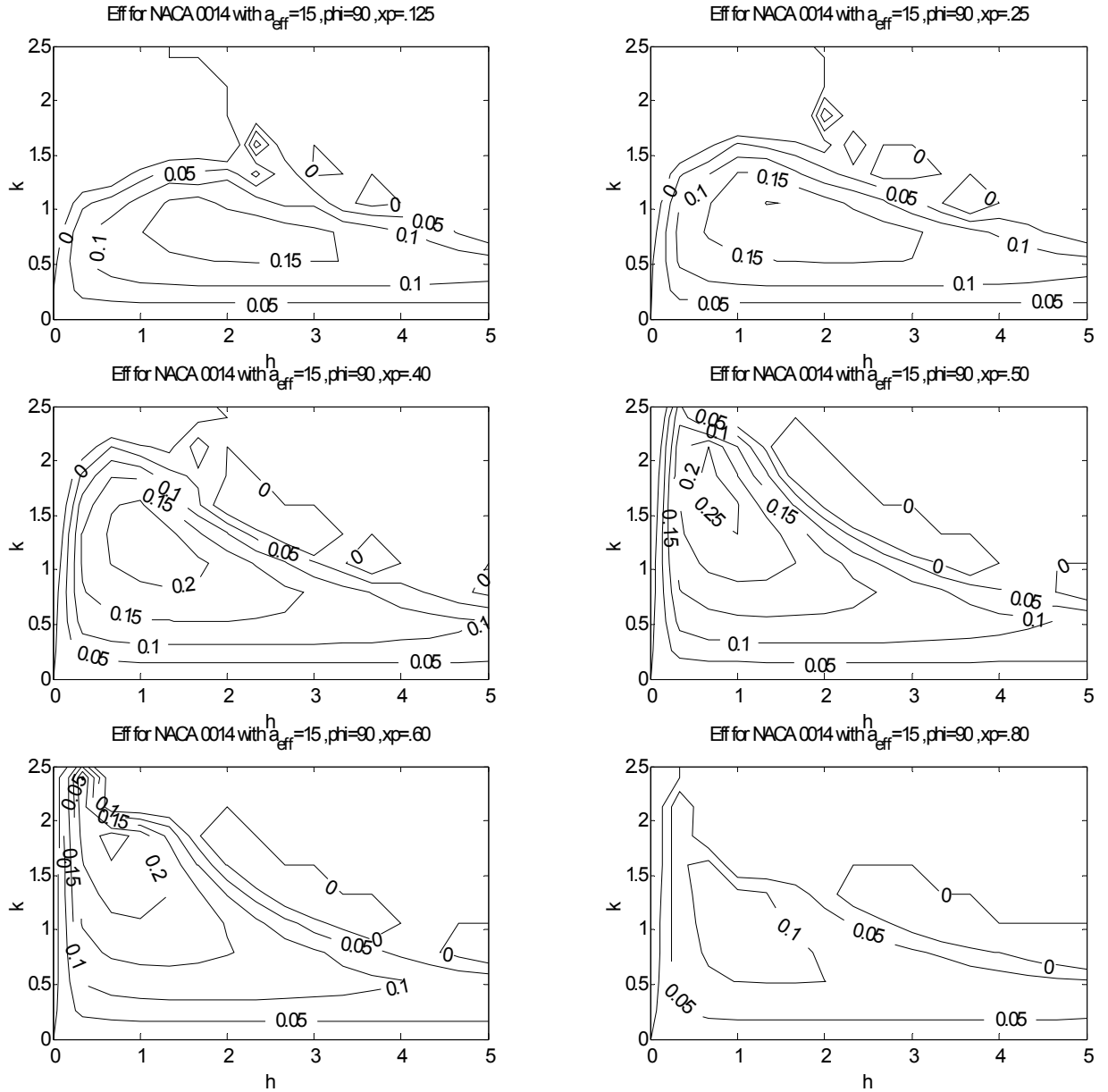result in reaching the requested effective angle. Consequently, this portion of the study yielded only trends rather than concrete numbers with which to work (i.e. the numbers displayed and used below are not to be taken individually but as a whole). The range of effective incidence angles studied was based on estimated stall angles.

As effective angle of attack grew from 10 to 20 degrees, power increased along with efficiency. Maximum power is extracted from the flow at low reduced frequency and higher plunge amplitudes, as seen in Figure 19.
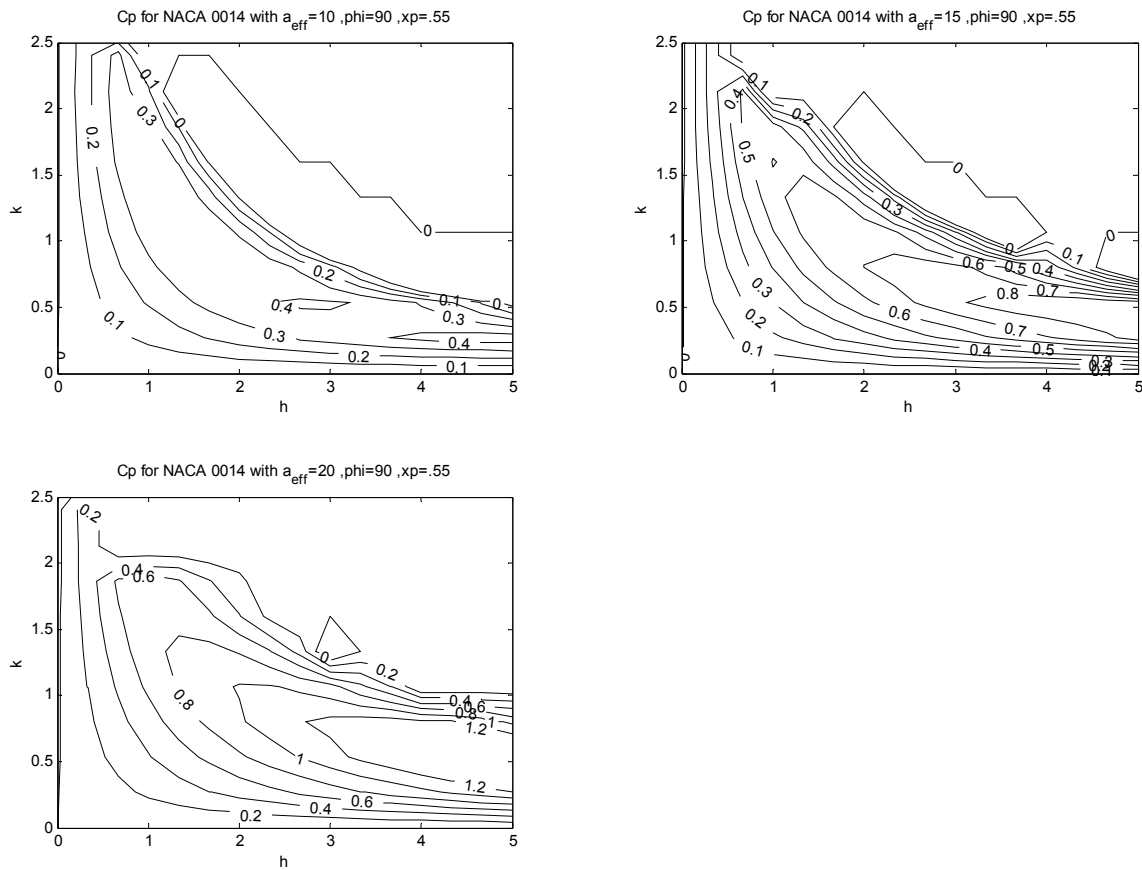


Figure 19.   Changes in Power with Effective Angle of Attack

Total efficiency improves as angle of attack increases, as is demonstrated in Figure 20. While this may seem somewhat intuitive since larger incidence angles mean taking a bigger "bite" out of the flow, it ignores separation losses. Also shown in the figure is that peak efficiency may be found at low plunge amplitude and higher reduced frequencies. Note that this position is in contrast to the location of peak power.
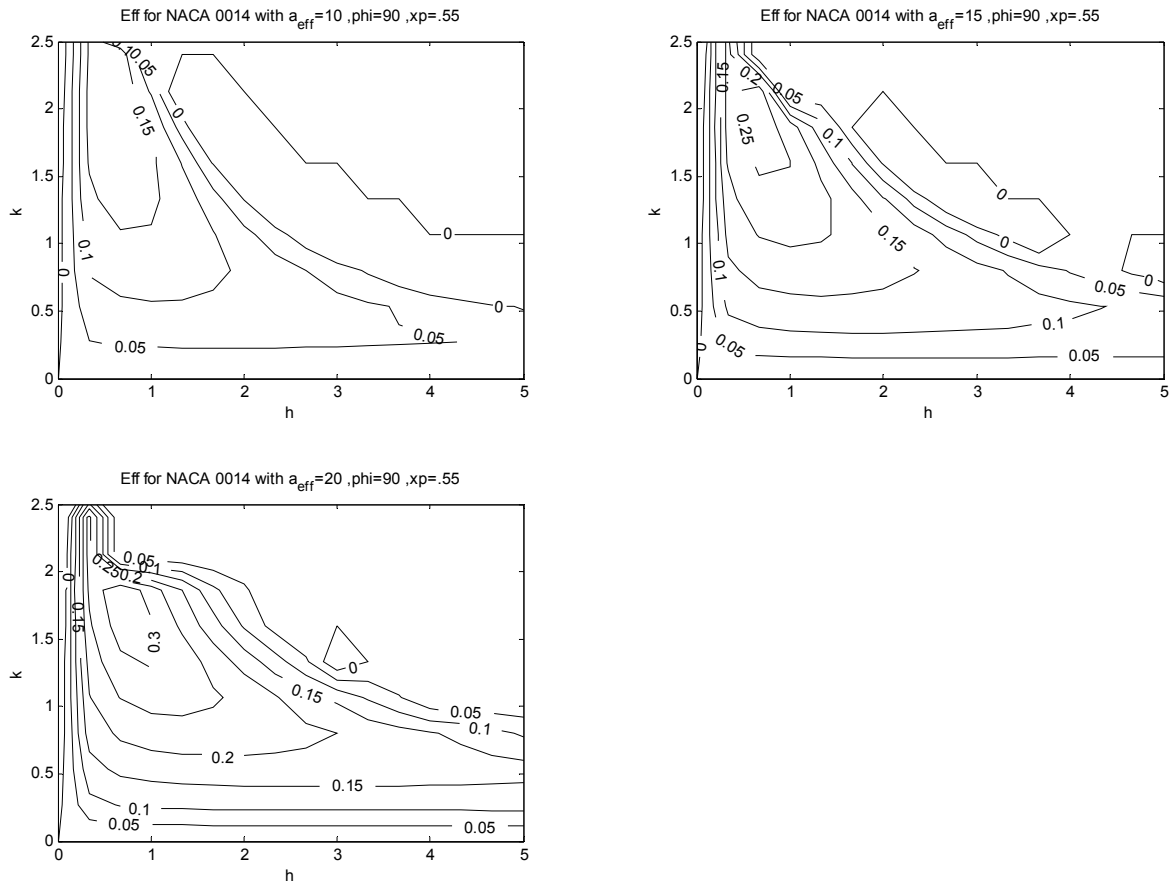


Figure 20. Changes in Total Efficiency with Effective Angle of Attack

### 4. Change in Airfoil Thickness

A point of interest, beyond the scope of this study, would be to determine what shape of airfoil could boost power output and/or efficiency from a wingmill. However, this study did briefly use UPOT to investigate if airfoil thickness might have some impact. Using standard NACA 00 series airfoils power and efficiency were computed and plotted for comparison. The results shown in Figure 21 reveal that at least for standard airfoils, thickness does have a measurable impact, if the flow actually stays

attached to the airfoil. It appears that a thinner airfoil can boost performance when comparing a NACA 0010, 0014, and 0018. However, the true test would come from a NS analysis since that will examine flow separation, which is greatly dependent on airfoil shape.



Figure 21.   Effect of Airfoil Thickness on Power Production

## 5.  Summary

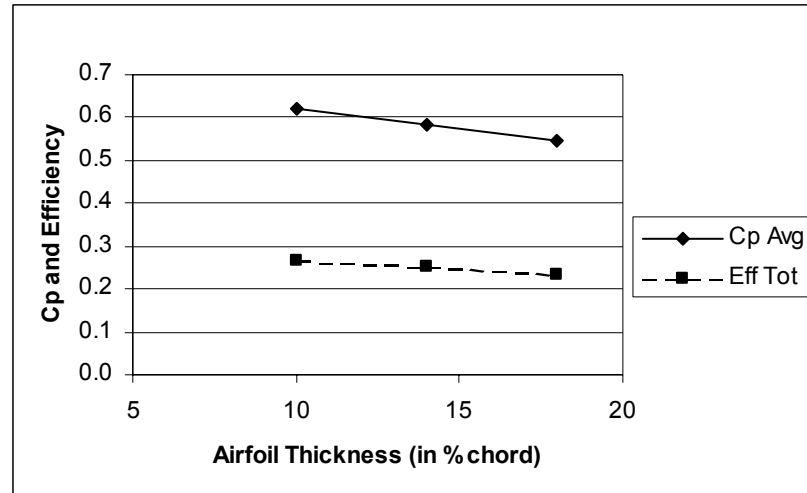A major result that UPOT helped point out is that maximum efficiency and power are often not found in the same location in the frequency-amplitude domain. Best total efficiency is generally seen at low plunge amplitudes and higher frequencies, however, best power is found at high amplitudes and lower frequencies. This is of utmost importance since it means that a wingmill cannot achieve maximum power and efficiency simultaneously, thus, its designers would have to choose which measurement is more important. When faced with this decision, it was helpful to know that current hydro-electric generators are built to obtain power out, as will be discussed later. Since this project was concerned with the practicality of an oscillating-wing generator, it became necessary to focus on conditions leading to the most power extracted.

Based on the data that UPOT supplied, it was determined that forward pivot point, phase angle of 90 degrees, and effective angle of attack at 20 degrees gave maximum power out. (UPOT predicts higher incidence angles to give better performance, but they are unrealistic since the flow will detach). It should be noted, however, that since

36

effective angle of attack cannot be predicted ahead of time, 15 degrees continued to be used as a basis for further calculations. The farthest forward pivot point for which calculations were done, 12.5% chord, gave its best performance at plunge amplitudes that the experimental generator was not capable of reaching. The next best power out came from a pivot at the quarter chord. This location actually provided more power in the device's capability range than a more forward chord, as shown in Figure 22. Compare *Cp* as a function of pivot point at *h* of 1 and 2. At *h* = 1, *Cp(12.5%)* peaks near 0.3 and *Cp(25%)* peaks near 0.4. Similarly, at *h* = 2, *Cp(12.5%)* peaks near 0.8 and *Cp(25%)* peaks just above 0.8. Thus, pivot point at the quarter chord was taken as the basis for the rest of the study.
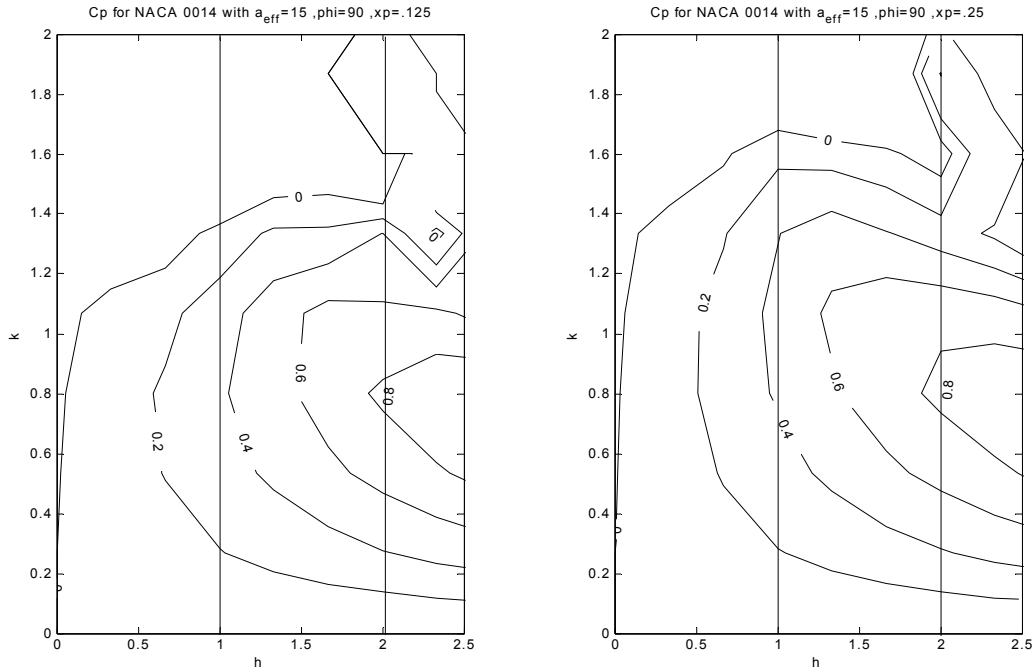


Figure 22.   Power at Pivot Points 12.5% and 25% Chord

**B.    NS**

As mentioned earlier, a Navier-Stokes analysis is computationally expensive and time consuming. Thus, seven points were chosen from the previously surveyed frequency-amplitude grid for evaluation. They were selected based on the ability of Jones' model to reach the operating parameters so that the results could be verified

experimentally. This study performed the NS analysis at Reynolds number of $10^6$ assuming fully turbulent flow to examine the wingmill in large-scale applications, and at Reynolds number $2 \times 10^4$, assuming fully laminar flow to model conditions in the water tunnel. The seven points were at $(h, k) = $ (1, 1), (1.3, 0.8), (1.3, 1), (1.3, 1.3), (2, 0.8), (2, 1), and (2.1, 1.3).

Each analysis began with finding a steady state solution for a stationary airfoil in a flow at the desired Reynolds number. This allowed start up transients to clear the vicinity of the airfoil before its oscillations began. The NS Code was then allowed to propagate for several cycles until the flow cleared the starting motion transients and showed periodicity. Finally, the outputted data was processed in a separate power conversion code developed by Jones. The results if individually presented would not convey much information other than what happens at a specific value of reduced frequency and plunge amplitude, therefore, they are presented for comparison with UPOT in the following section.

## C.    COMPARISON OF NUMERICAL RESULTS

From previous knowledge of flapping-wing propulsion, it was anticipated that UPOT and the high Reynolds number Navier-Stokes case would yield significantly better performance than the low Reynolds number case and this proved to be correct. UPOT predicts better performance because of the approximations that result from the assumptions used in the Laplace equation. At a Reynolds number of $10^6$, flow is assumed fully turbulent and many difficulties that may arise from viscosity do not hinder performance. Thus, at higher Reynolds numbers an oscillating-wing generator actually should produce more power. The low Reynolds number NS results indicated what was believed to be a closer representation of what could be expected from the water tunnel test. Power and efficiency from the computational models are summarized in Table 1, with the "Efficiency" column showing efficiency based on drag for comparison. The models generally show that a noteworthy amount of power can be produced. High total efficiencies result from maximizing disturbances in the flow (i.e. high drag) whereas the

low total efficiencies indicate that much of the power in the flow remains unextracted. This is typical for hydro and wind power generators.

Table 1. Power Prediction Summary

| h=1.0, k=1.0 | Cp | Efficiency | Total Efficiency |
|---|---|---|---|
| UPOT | 0.4524 | 0.5672 | 0.1819 |
| N.S. 1x10^6 | 0.5995 | 0.5980 | 0.2410 |
| N.S. 2x10^4 | 0.4108 | 0.4697 | 0.1652 |

| h=2.0, k=0.8 | Cp | Efficiency | Total Efficiency |
|---|---|---|---|
| UPOT | 0.8438 | 0.6614 | 0.1919 |
| N.S. 1x10^6 | 1.2337 | 0.7479 | 0.2805 |
| N.S. 2x10^4 | 0.7427 | 0.5579 | 0.1689 |

| h=1.3, k=0.8 | Cp | Efficiency | Total Efficiency |
|---|---|---|---|
| UPOT | 0.5605 | 0.6946 | 0.1859 |
| N.S. 1x10^6 | 0.7155 | 0.7393 | 0.2373 |
| N.S. 2x10^4 | 0.4852 | 0.5942 | 0.1609 |

| h=2.0, k=1.0 | Cp | Efficiency | Total Efficiency |
|---|---|---|---|
| UPOT | 0.8323 | 0.4891 | 0.1872 |
| N.S. 1x10^6 | 1.4833 | 0.6421 | 0.3336 |
| N.S. 2x10^4 | 0.6879 | 0.3963 | 0.1547 |

| h=1.3, k=1.0 | Cp | Efficiency | Total Efficiency |
|---|---|---|---|
| UPOT | 0.6138 | 0.5693 | 0.1990 |
| N.S. 1x10^6 | 0.8355 | 0.6302 | 0.2709 |
| N.S. 2x10^4 | 0.5317 | 0.4707 | 0.1724 |

| h=2.1, k=1.3 | Cp | Efficiency | Total Efficiency |
|---|---|---|---|
| UPOT | 0.3109 | 0.1194 | 0.0663 |
| N.S. 1x10^6 | 1.3716 | 0.3831 | 0.2926 |
| N.S. 2x10^4 | 0.1085 | 0.0362 | 0.0231 |

| h=1.3, k=1.3 | Cp | Efficiency | Total Efficiency |
|---|---|---|---|
| UPOT | 0.5394 | 0.3373 | 0.1708 |
| N.S. 1x10^6 | 0.9956 | 0.4421 | 0.3152 |
| N.S. 2x10^4 | 0.3500 | 0.1931 | 0.1108 |

Notice from the table that for all values of *h* and *k* that the high Reynolds number estimations were significantly greater than the other two—on the order of 30% greater and upwards. This large difference necessitated investigating what was happening in the flow between the two models, as will be described below. Notice also in Table 1 that UPOT's predictions for $C_p$ and total efficiency are relatively close, within about 10%, of the low Reynolds number NS case. This is coincidental since UPOT and NS are predicting quite different physics.

To determine why UPOT and the NS Reynolds number $10^6$ case differed as much as they did, the study turned to flow visualization. In Figure 23, half a cycle of airfoil oscillation is displayed from UPOT at *k*=0.8 and *h*=1.3. Flow velocity profiles are to the right. Nothing unusual was detected as a discrete vortex was shed from the airfoil's trailing edge (recall, UPOT does not allow separation except at the trailing edge) at the bottom and top of the plunge cycle. Since UPOT yielded no indications of abnormalities, the search now turned to the NS results in Figures 24 and 25.
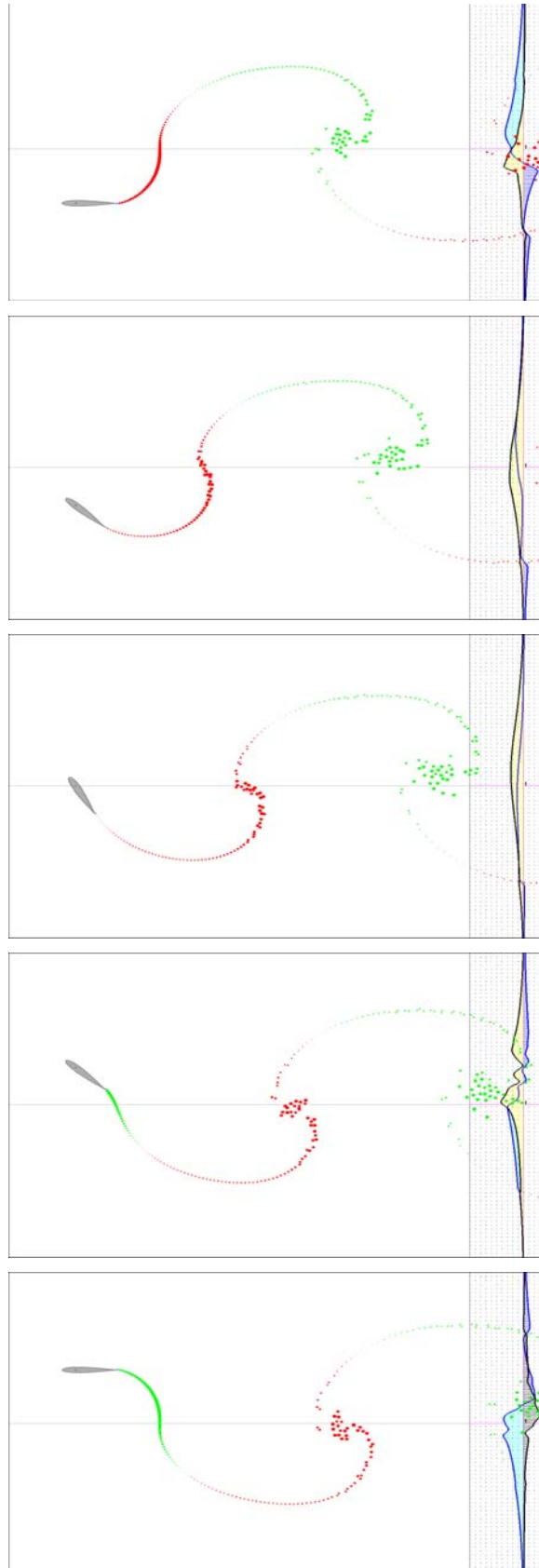
Figure 23.   UPOT Display of Oscillating Airfoil Impact on Flow at *k*=0.8 and *h*=1.3

Streaklines, vorticity distribution, and wall velocities resulting from flow at the high Reynolds number are displayed in Figure 24. The sequence shows the airfoil traveling from minimum to maximum plunge for an effective angle of attack of 15 degrees. A continuous vortex sheet is shed because of the incessant change in angle of attack. Notice that the flow seems to remain attached throughout the cycle, so this allows a fair comparison to UPOT. Two phenomena which may help account for the better performace at NS high Reynolds number include a possible difference in the magnitude of vorticity and the beginnings of what may be a "separation bubble" in the NS analysis. This possible region of reverse flow is seen as a dark spot on the upper surface of the airfoil in the 4th and 5th frames. Flow velocity vectors to the right of each frame remain fairly constant throughout the sequence indicating relatively small disturbances, which helps to explain why this case has higher drag based efficiencies that were related in Table 1.

Streaklines, vorticity distribution, and wall velocities resulting from flow at the low Reynolds number are displayed in Figure 25. Again, the sequence shows the airfoil traveling from minimum to maximum plunge. It is immediately apparent in the sequence that the airfoil is stalled through most of the cycle. This reveals that the 15 degree effective angle of attack is too much for the low Reynolds number condition, and confirms the reasoning for reduced performance with respect to the first NS model.
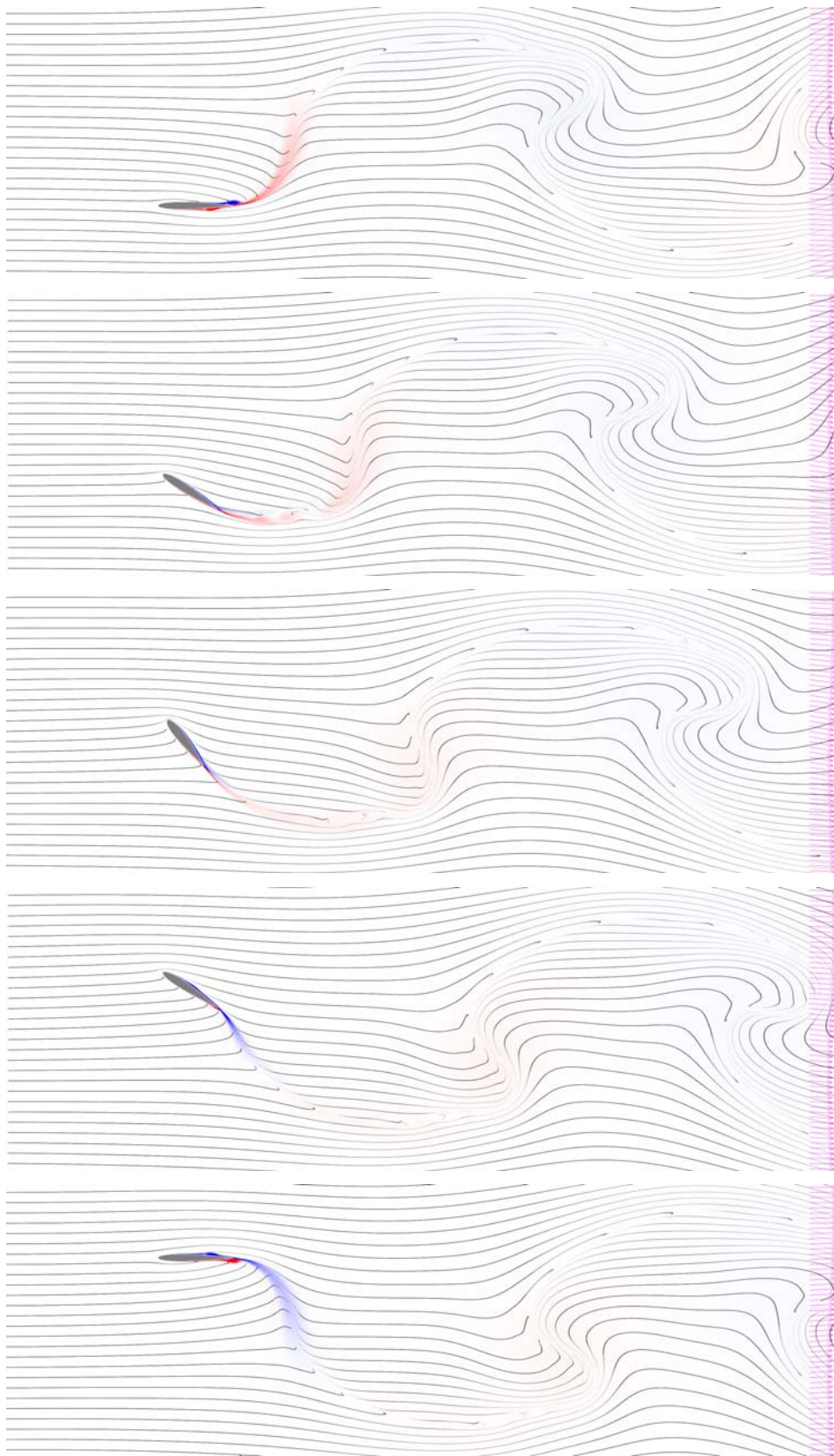
Figure 24. NS $Re$=10$^6$ Oscillating Airfoil Streaklines at $k$=0.8 and $h$=1.3
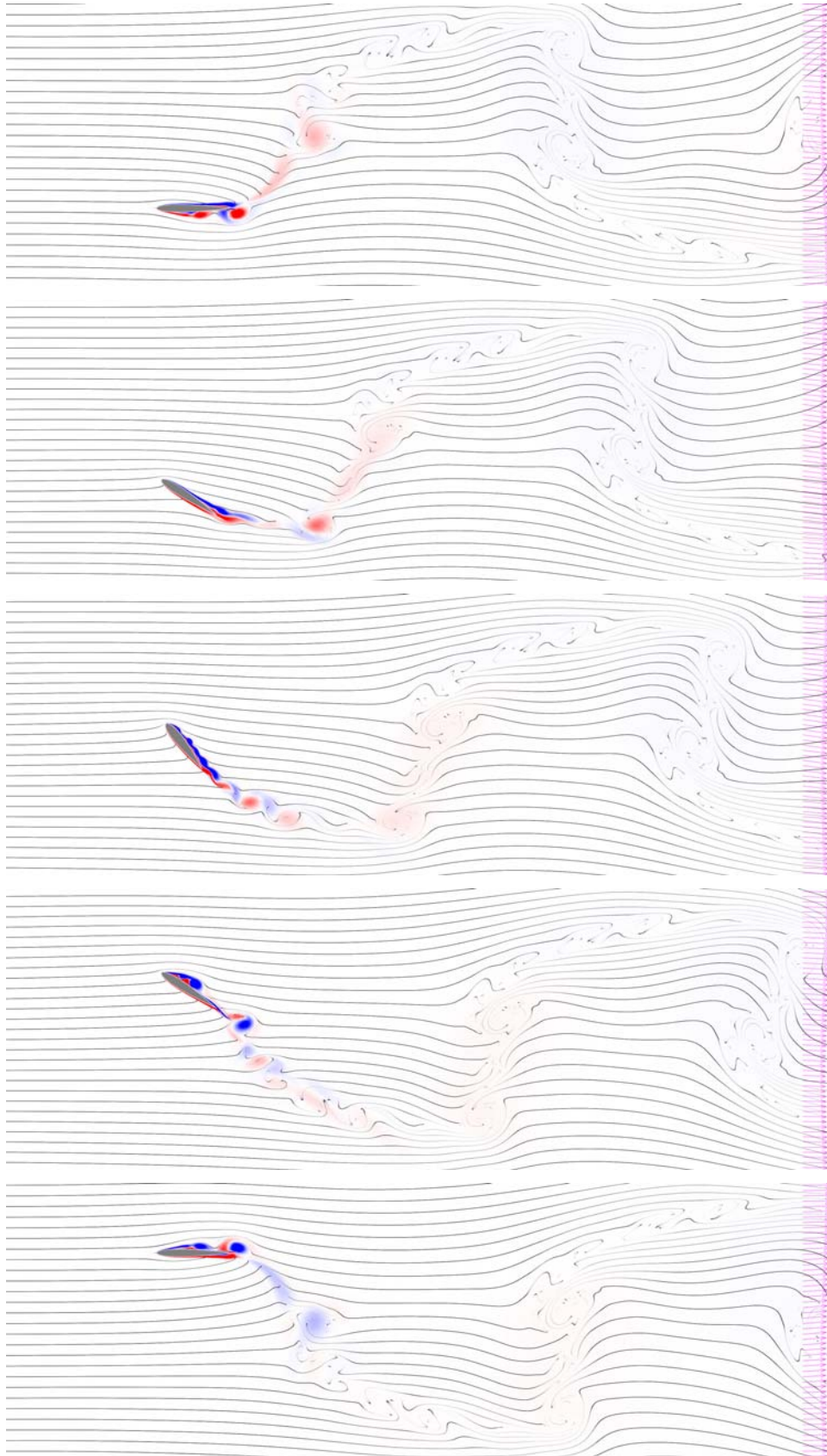
Figure 25.   NS $Re$=2x10$^4$ Oscillating Airfoil Streaklines at $k$=0.8 and $h$=1.3

THIS PAGE INTENTIONALLY LEFT BLANK

## VI.  EXPERIMENTAL RESULTS

The results of testing the experimental oscillating-wing generator proved that the apparatus could in fact produce measurable quantities of power.  They also validate the concept of such a generator as a power production device.  However, the quantities of energy extracted will call into question the generator's practicality.   This will be discussed in Section VII.

In the following graphs $C_p$ is plotted against reduced frequency.  Geometric angles of attack are indicated for the neutral plunge position.  Experimental results are separated by angle of attack with the first set being for a plunge amplitude of 1.05 times the airfoil chord.  As seen in Figures 26 and 27, as geometric angle of attack increases so does the power extracted.  The higher angles allow the airfoil to take a larger "bite" out the flow.
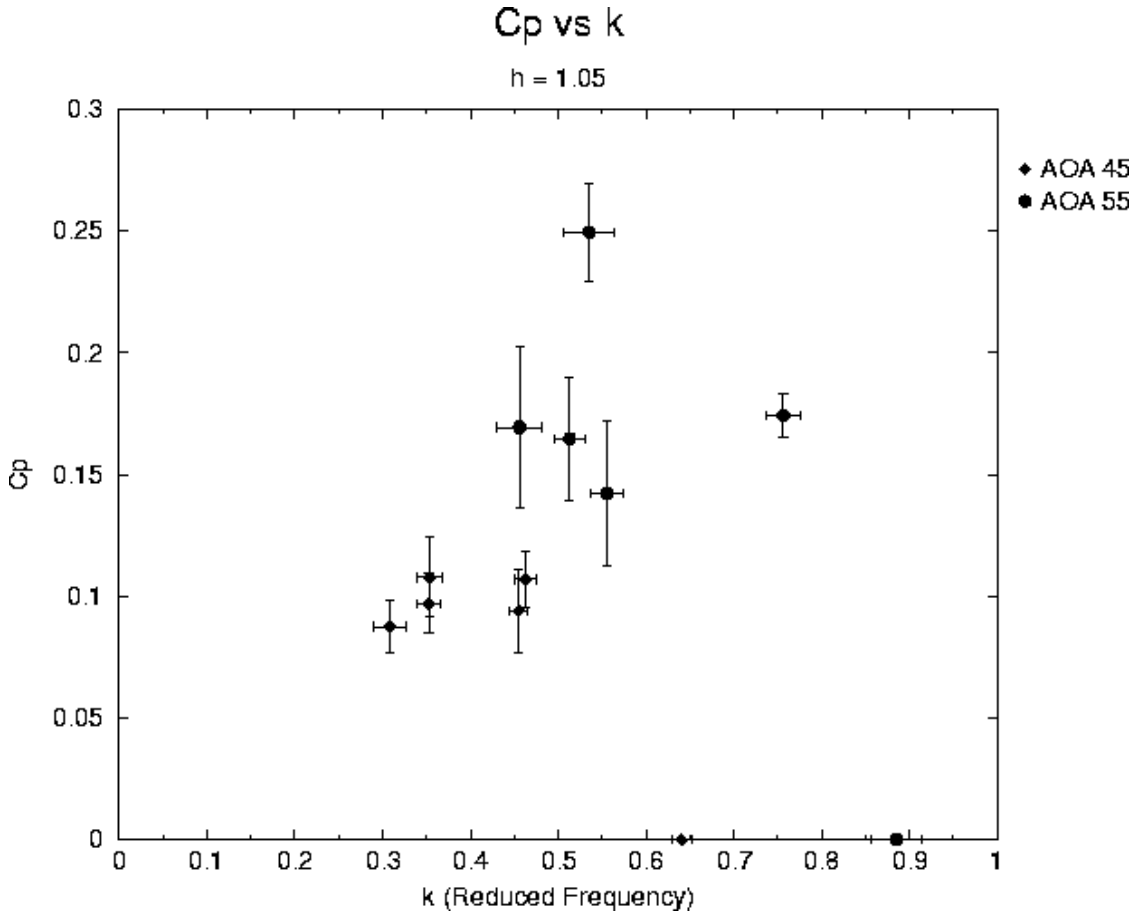


Figure 26.   Power vs. Frequency for Plunge Amplitude of 1.05, lower AOA
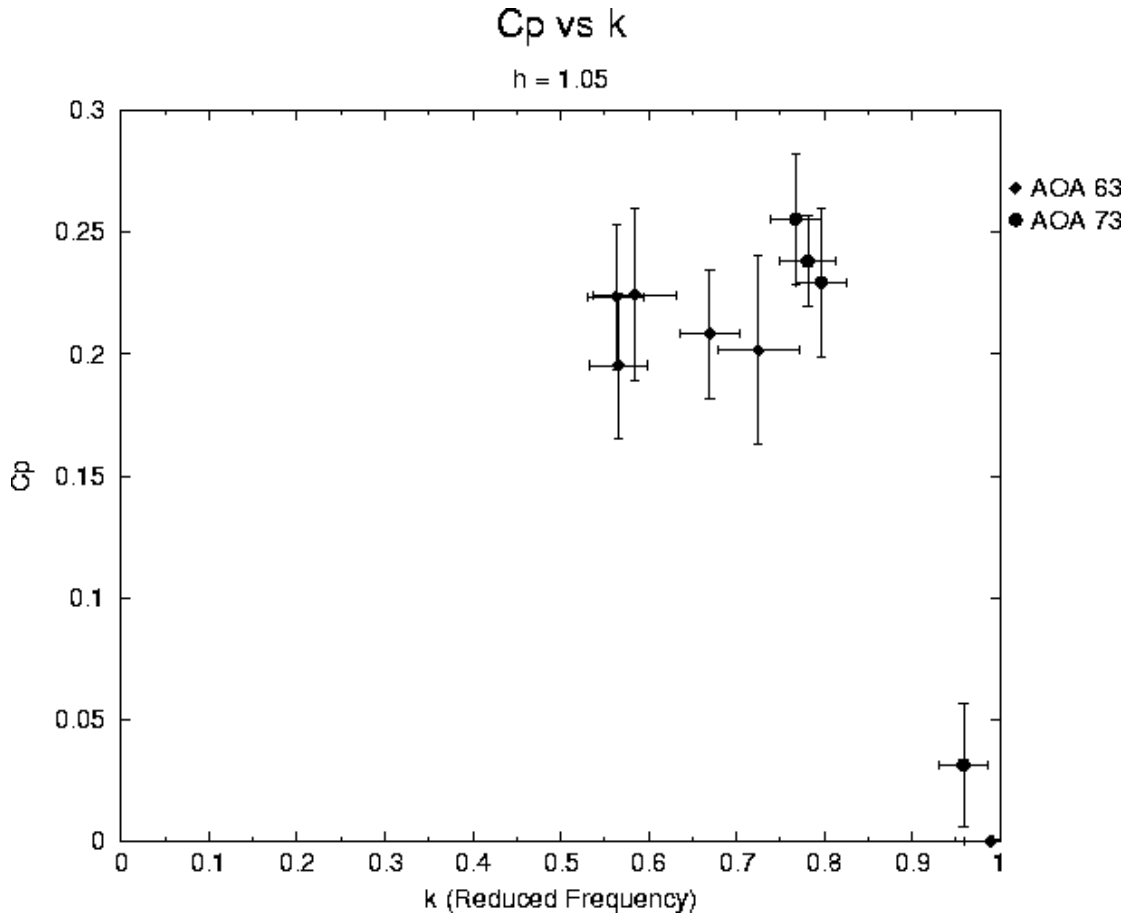
45

Figure 27.   Power vs. Frequency for Plunge Amplitude of 1.05, higher AOA

In actuality, higher angles create more lift (up until and perhaps stall) to force airfoil motion.  At *h* = 1.05 peak power is seen in Figure 27 at 73 degrees angle of attack near *k* = 0.77.  The effective attack angle at this point is 38 degrees (from Equation 5), well past stall, yet there is ample power produced.   McKinney and DeLaurier noted the explaniation for this counterintuitive result, "airfoil normal forces dominate in the power-production, with only second-order effects from leading edge suction."  [Ref. 1]  Thus, even with stall an airfoil is capable of extracting power.  Notice also that points on the horizontal axis indicate the maximum oscillation frequency, which corresponds to no load being imposed on the generator.  In all of the experiments, effective varying angle of attack decreased as frequency increased (as anticipated from Equation 11).

Also pictured in Figures 28 and 29 is power increasing with pitch amplitude for plunge amplitude of 1.31.  No-load cases demonstrating peak frequency are seen on the

46

horizontal axes, as well. Similar to the lower plunge amplitude cases, the maximum angle of attack yielded the highest $C_p$. This is seen in Figure 29, where 73 degrees angle of attack produced a $C_p$ of more than 0.2. Effective angle of attack here is 31 degrees, again, past stall but still producing power, thus, confirming the earlier observation and statement by McKinney and DeLaurier.



Figure 28.   Power vs. Frequency for Plunge Amplitude of 1.31, lower AOA
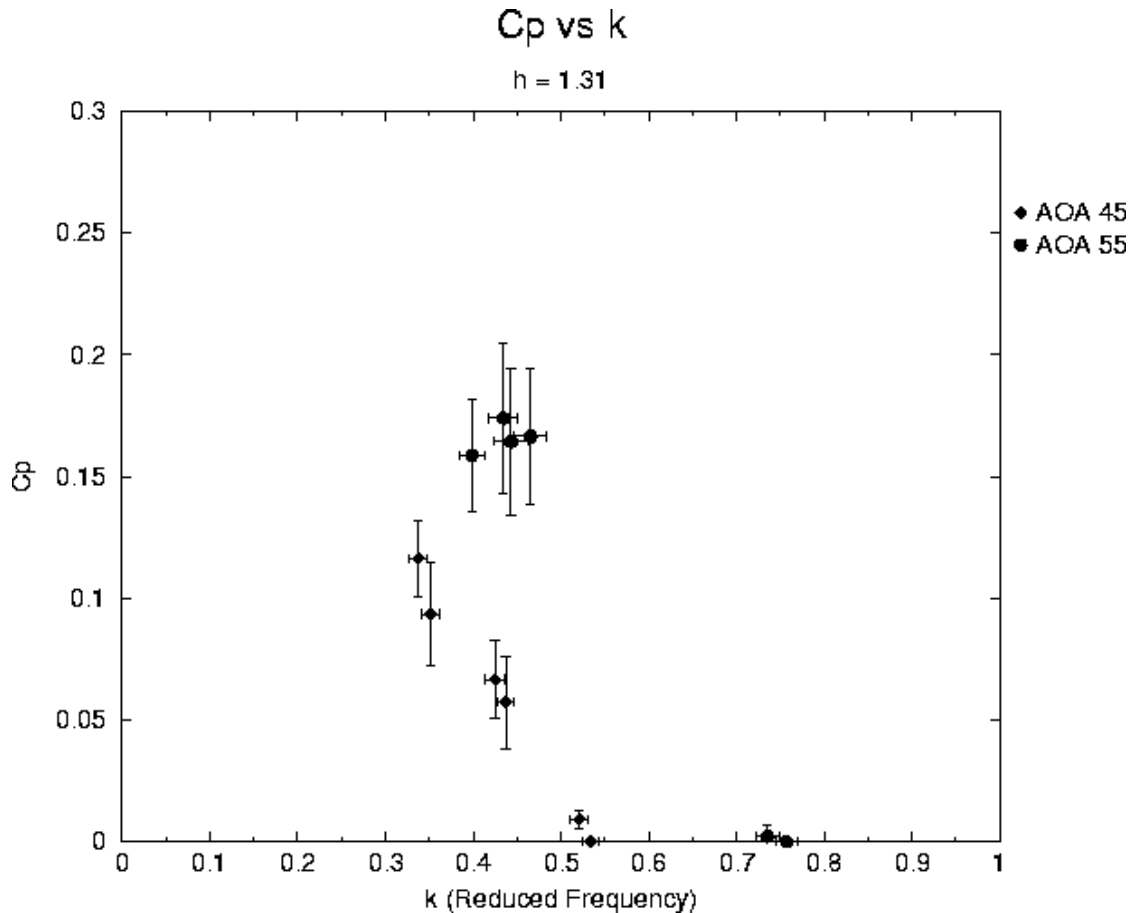
That the higher plunge amplitude produces less power than the experiments with $h$=1.05 was not expected. According to the numerical analysis, higher plunge amplitude, since a greater area is swept out, should yield greater power. Perhaps the experimental difference is due to inertial effects from having to accelerate the rocker arms over a longer distance.
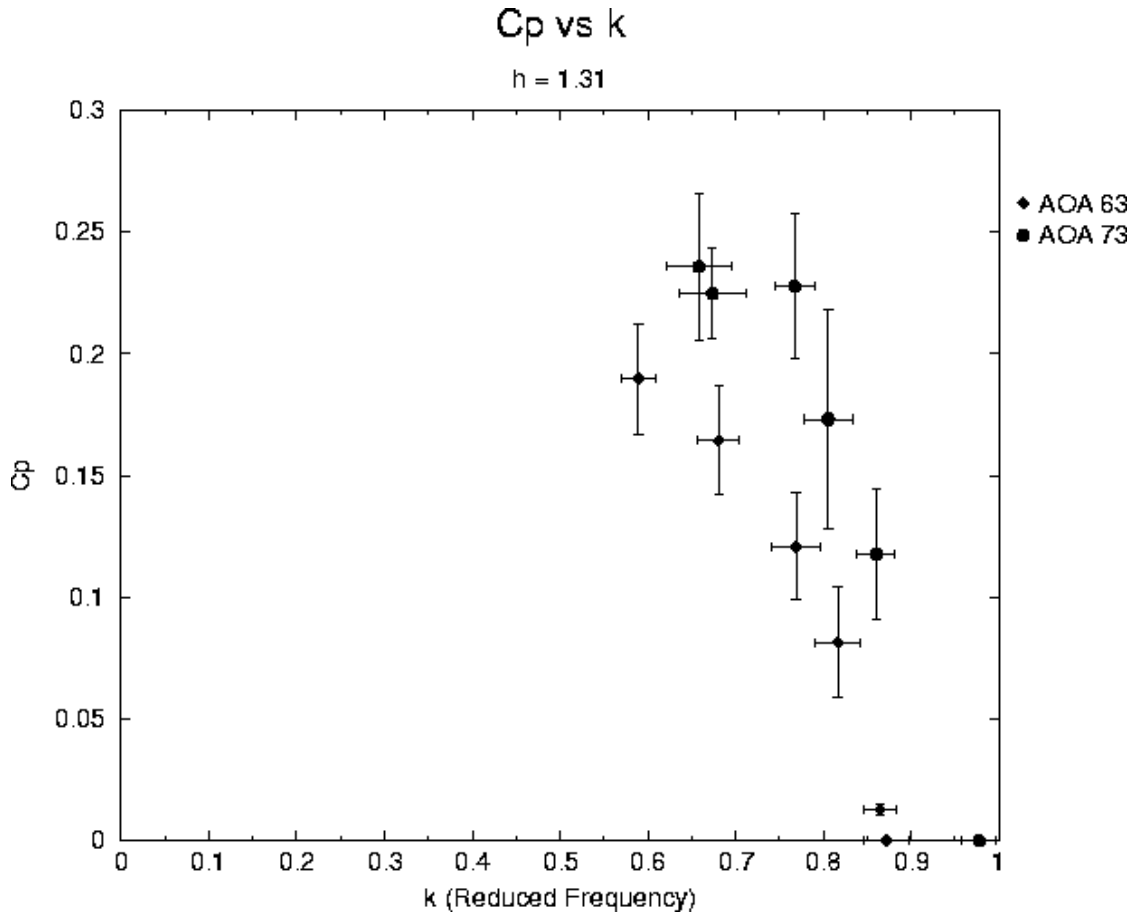
47

Figure 29.   Power vs. Frequency for Plunge Amplitude of 1.31, higher AOA


Peak total efficiencies are summarized in Table 2, with the indicated powers in Watts.  The actual total efficiency achieved was on par with McKinney & DeLaurier and Davids, being in the teens of percent.  Predicted total efficiency (from Table 1), near one third, confirms Davids numerical models, as well.  Equipment for measuring drag was not available in the water tunnel so no analysis of drag-based efficiency was made.


Table 2.     Experimental Total Efficiencies

| Test Case | Max Power Out (Watts) | Available (Watts) | Total Efficiency |
|---|---|---|---|
| h=1.05 (Cp=0.25) | 0.31 | 1.34 | 0.23 |
| h=1.31 (Cp=0.23) | 0.28 | 1.68 | 0.17 |

# VII.  COMPARISON OF RESULTS


A comparison of numerical and experimental results was at first surprising in how much they differed.  Numerical analysis predicted much higher power levels should have been reached when an oscillating-wing generator was put to the test.  However, upon reflection of the differences between the physics of the two, there is not really anything out of the ordinary.  For example, the numerics were considering two-dimensional flow, whereas, in reality the flow had three dimensions.  Also, NS and UPOT did not analyze the velocity deficit impinging upon the second wing.  Recall the aft wing only had 16/27 of the remaining power available in the flow after the first wing had extracted its portion.  Additionally, in the NS code the airfoil under consideration was forced to maintain a preset frequency and plunge amplitude.  This prevented it from experiencing the full effects of stall, such as, being able to cease motion when there was not enough normal force to propel it.  Taking the differences between modeling and reality into account allows one to view their varying results with a proper perspective.

The gap in $C_p$, is depicted in Figure 30 where the predicted values are some 200% greater than the measured.  This graph covers the lower angle of attack region for the test model.  Recall from the previous section that lower angle tests yielded their power at $k$ of less than 0.5.  Thus, it is shown that the numerical modeling also forced higher operational frequencies where peak power occurred.  Note that in Figures 30 and 31 the NS data are for the low Reynolds number solutions.
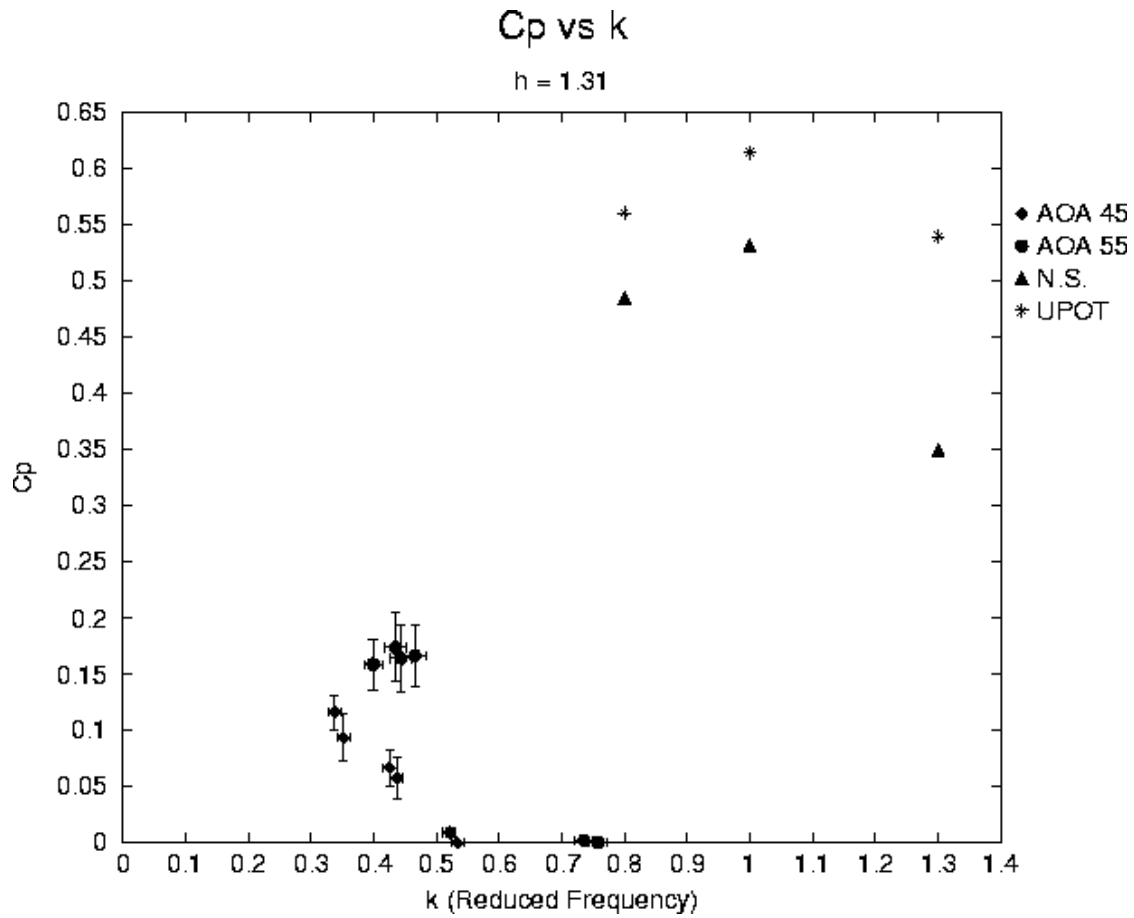
Figure 30.   Power Summary of Numerical and Experimental Results for lower AOA

Figure 31 is a summary of results that includes the higher angle of attack data. Recall that operation at these incidence angles yielded slightly more power than lower ones, so it is reasonable that these experimental results are closer, although still far off, to the predicted values.  Again the difference is on the order of 200% between the numerical and experimental quantities.  It is noteworthy that not only do higher airfoil amplitudes yield more power, they operate at higher reduced frequencies.  However, effective angle of attack decreases as higher frequencies are reached (predicted by Equation 11) delaying the onset of stall.  This may contribute to higher performance past the anticipated stall point by wingmills.
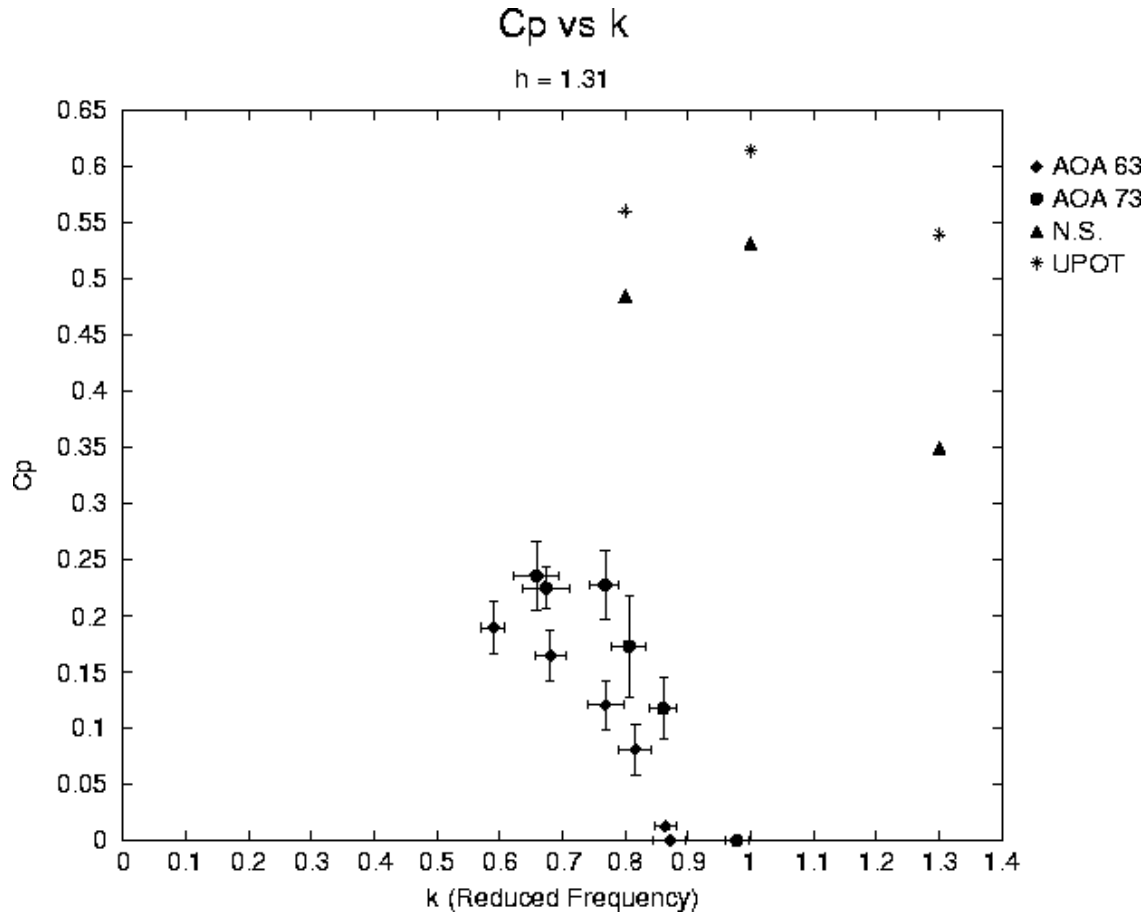
Figure 31.   Power Summary of Numerical and Experimental Results for higher AOA

The frequency of model operation is a point of interest since, in spite of the data disparity, the experiment did indicate that if a physical model could approach the predicted frequencies, it could also approach the forecast power output. A careful examination of Figures 30 and 31 will confirm this statement as the performance region shifts from Figure 30 upward and to the right in Figure 31. This is in the direction of the predicted performance zone.

For a physical perspective on these results power output for two sample values of $C_p$ are displayed in Figure 32. The lower value is representative of what the experimental generator could extract during the water tunnel test. As seen, at $C_p$=0.25 the generator could provide 0.31 Watts, although at a predicted $C_p$ of 0.4 it should have been able to give 0.5 Watts.
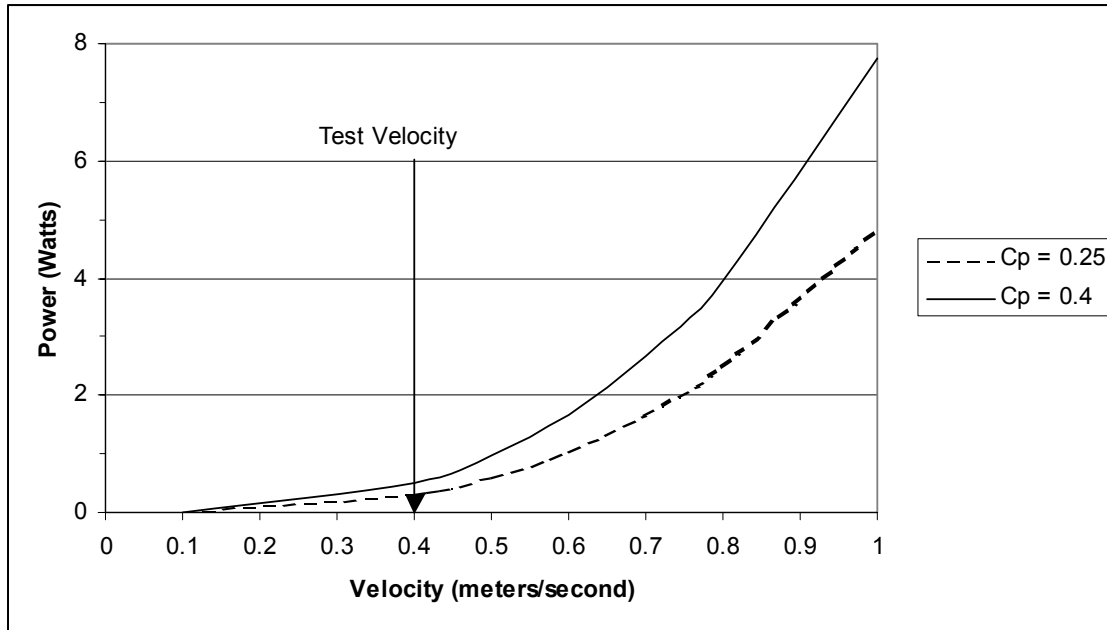
Figure 32.   Physical Power Output from nondimensionalized Powers

Now the question remains, why did the test generator not live up to expectations? Certainly several factors contributed to these results, as discussed in the sources of error, although how much is not known and may be the object of future studies. Among them was the quality of the airfoils on the generator. They were made of wood and while coated with a water resistant covering, water was still able to cause some nonuniformities by seeping in through attachment points and blemishes. Mechanical inertia required the use (loss) of power for the continuous change of direction for oscillating airfoils. Also, friction in the gears and pulleys dissipated energy extracted from the water flow. Another reason for differences in performance can be traced to the assumption of laminar flow at the low Reynolds number. Defects in the wings almost certainly invalidated that assumption. There was a trivial difference in tunnel Reynolds number from the numerical models, however, other factors figured more prominently into the mystery. Some of these concerns are modeling the finite span, split between the wing segments, interference between wings, and the effort required to drag the model's rocker arms through the water. These challenges must be addressed before an oscillating-wing generator can be introduced for widespread commercial applications. Yet, even at this stage in its development, such a generator holds positive potential.

# VIII. COMMERCIAL APPLICATIONS

The major thrust of this study was to determine if an oscillating-wing generator was feasible for commercial use, large scale or small. The Energy Information Administration's 1997 Residential Energy Consumption Survey reported that U.S. households used an average of 101 million BTU (29,593 kW-hr) per year. [Ref. 11] That translates into 3.378 kW per hour. A personal oscillating-wing generator operating at the demonstrated $C_p$ of 0.25 could power such a home if it had wings with total area of 0.5 square meters and were placed in a 3.7 meter per second flow, that is if the electrical conversion process had negligible losses. If such a generator were able to reach the predicted $C_p$ of 0.4, the same energy could be provided by a 3.2 meter per second flow. Naturally, an energy efficient home would use much less energy and require a smaller generator or lower flow speeds.

Certainly those houses that were not located near a river or stream could not take advantage of a personalized oscillating-wing generator. However, for those that are, hydroelectric generators are already available that are designed for partial home power provision. A representative model is the Aquair 12Volt Underwater Turbine Generator, which produces 100 Watts in a fast stream (about 4 meters per second) at a unit cost of near $1000. [Ref. 12] Jones' generator is capable of far exceeding that output with its current airfoil size, as seen in Figure 33, and is more likely to be a total power provision source. It should also be noted that oscillating-wing generators are, thus far, more efficient than such personal generators. The Aquair with a propeller diameter of 312 mm only extracts 100 Watts out the 2400 available from a 4 meter per second stream flowing through its blades. That equates to 4% total efficiency compared to the wingmill's 17-23%. Mass production cost of oscillating-wing generators is not currently known. So in spite of its inability to meet predicted expectations, the test model is very competitive for power output in the "micro hydroelectric" generator market.
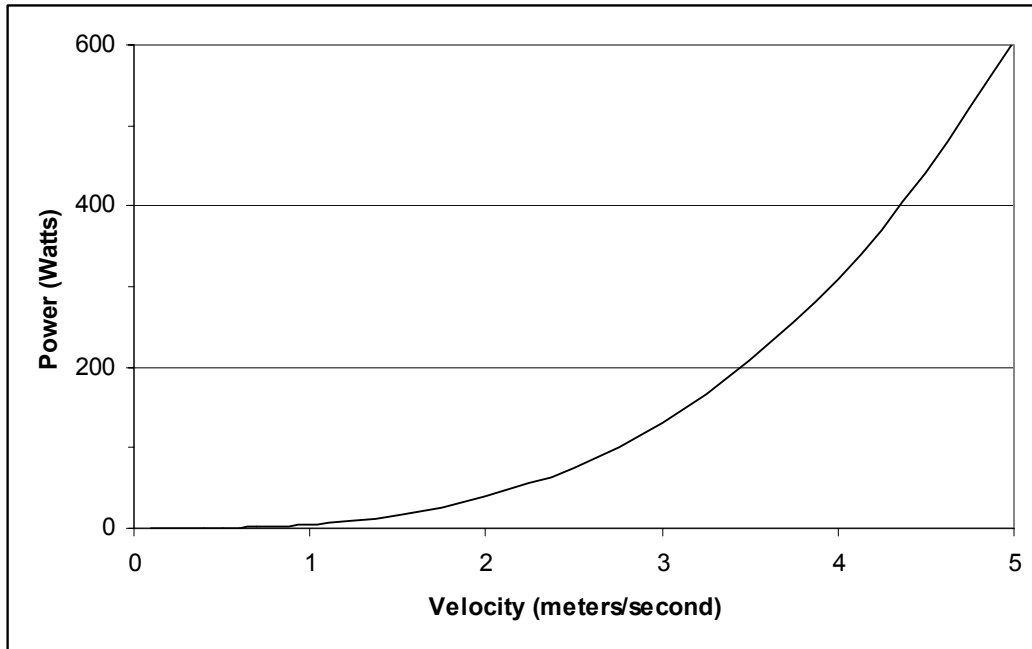
Figure 33.   Micro Hydroelectric Generator Power Production, Jones' Model

What are the possibilities for oscillating-wing generators in large-scale applications?  Consider a generator placed between the columns of a bridge over a river. The power output for a tandem wing generator with total wing area of 20 square meters is shown in Figure 34.  Typical Reynolds numbers for such wings (of one meter chord) would range from 5 to 8 million at river speeds between 3 and 5 meters per second. Natural river flow velocities are usually too low to enable large amounts of power to be extracted, however, venturies funneling and accelerating water toward a generator can enable speeds to be reached that yield practical amounts of power.  Several generators may be placed under a single bridge to multiply the energy available for commercial consumption.
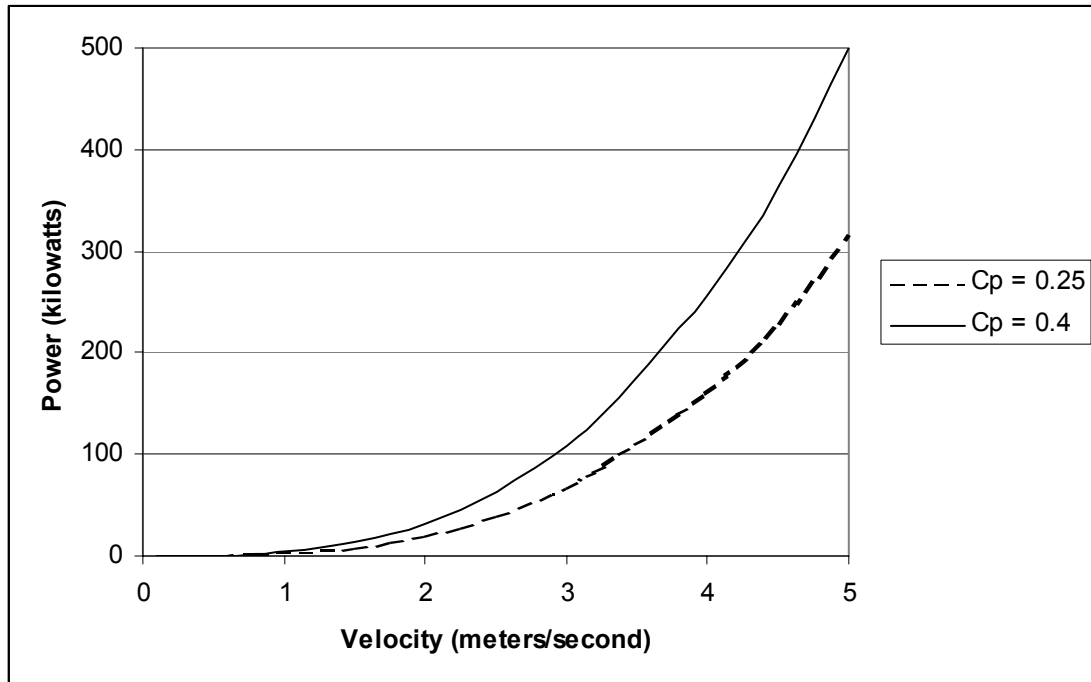
Figure 34.   Hydroelectric Generator Power Production with known and potential capabilities.


What advantages does an oscillating-wing hydroelectric generator have over conventional ones?   Primarily, they do not necessitate a change of landscape and environment for construction or operation.   This new class of power producer can be placed in many locations where dams and conventional hydro power plants cannot. They may even be made in portable units that can be shifted from place to place along a river.   However, existing hydroelectric power plants need not be dismantled because oscillating-wing generators may simply be added downstream to extract more energy.

THIS PAGE INTENTIONALLY LEFT BLANK

# IX. CONCLUSIONS

For modern man, renewable and zero-pollution energy supplies are of great interest. In the quest for clean sources of energy, new methods to harness known sources must be seriously considered. Consequently, power generation from a fluttering wing has been studied numerically and experimentally. Previous studies that suggested an oscillating-wing might be used to extract energy from a fluid flow have been examined and validated by numerical and experimental means. A model oscillating-wing generator was designed, tested, and found workable although it did not meet expectations based on preliminary numerical modeling. Even with limited power production discerned in this study, oscillating-wing generators have potential for commercial use, especially if the performance of the numerical models can be reached.

THIS PAGE INTENTIONALLY LEFT BLANK

# X. RECOMMENDATIONS

Based on the information discerned and presented in this study, wingmills have a large potential in the energy production market. However, they have several challenges yet to be overcome. Foremost among these issues is why the generators previously tested, including the one from this study, do not match the power output predicted by numerical modeling. The need for better numerical models has been made apparent in the discussion of this study, chiefly one with ability to obtain a non-forced frequency of oscillation, account for inertial effects, and damping, as well. Improved models should be foremost in future studies. The related topic is then how to build a generator that approaches or matches the numerical power predictions. Future studies will also need to consider the environmental impact of extracting large amounts of energy from rivers should series of wingmills ever be used, and the cost to build them.

THIS PAGE INTENTIONALLY LEFT BLANK

# LIST OF REFERENCES

1. McKinney, W. and DeLaurier, J., "The Wingmill: An Oscillating-Wing Windmill," Journal of Energy, Vol. 5, No. 2, March-April 1981, pp. 109-115.

2. Jones, K. D. and Platzer, M. F., "Numerical Computation of Flapping-Wing Propulsion and Power Extraction," AIAA Paper No. 97-0826, Reno, NV, January 1997.

3. Davis, S. T., "A Computational and Experimental Investigation of a Flutter Generator", Master's Thesis, Naval Post Graduate School, Monterey, CA, June 1999.

4. Anderson, J. D., *Fundamentals of Aerodynamics*, 2nd edition, McGraw-Hill, Inc. New York, 1991, pp. 16-17.

5. Young, W. C., *Roark's Formulas for Stress & Strain*, 6th edition, McGraw-Hill, Inc. New York, 1989, p. 5.

6. Platzer, M. F., Class Lecture Notes, Naval Post Graduate School, Monterey, CA, 2002, pp. 11-13.

7. Teng, N., "The Development of a Computer Code (U2DIIF) for the Numerical Solution of Unsteady, Inviscid and Incompressible Flow Over an Airfoil", Master's Thesis, Naval Post Graduate School, Monterey, CA, June 1987.

8. Ekaterinaris, J. A. and Menter, F. R., "Computaiton of Oscillating Airfoil Flows with One- and Two-Equation Turbulence Models," AIAA Journal 32, 1994, pp. 2359-2365.

9. Holman, J. P., *Experimental Methods for Engineers*, 7th edition, McGraw-Hill, Inc. New York, 2001, p. 470.

10. White, F. M., *Fluid Mechanics*, 2nd edition, McGraw-Hill, Inc. New York, 1986, pp. 673-675.

11. Energy Information Administration, "Change in Energy Usage in Residential Housing Units" http://www.eia.doe.gov/emeu/recs/recs97/decade.html#totcons2, September 2002.

12. ABS Alaskan, "Product Information" http://www.absak.com/cgi-bin/shop/search.cgi?user_id=15592&database=db_main.txt&template=item.htm&0_option=1&0=AQUW, September 2002.

THIS PAGE INTENTIONALLY LEFT BLANK

# INITIAL DISTRIBUTION LIST

1.      Defense Technical Information Center
        Ft. Belvoir, Virginia

2.      Dudley Knox Library
        Naval Postgraduate School
        Monterey, California

3.      Major Scott T. Davids, USMC
        U.S. Naval Academy Aerospace Dept
        Annapolis, Maryland

4.      Professor Max Platzer
        Naval Postgraduate School
        Monterey, California

5.      Professor Kevin Jones
        Naval Postgraduate School
        Monterey, California